CENTRO DE INVESTIGACIÓN Y DE ESTUDIOS AVANZADOS DEL INSTITUTO POLITÉCNICO NACIONAL

UNIDAD ZACATENCO

DEPARTAMENTO DE FARMACOLOGÍA

"Role of beta4 subunit of L-type calcium channels as a regulator of transcription in heart"

TESIS

Que presenta

Eshwar Reddy Tammineni

Para obtener el grado de

DOCTOR EN CIENCIAS

EN LA ESPECIALIDAD DE

FARMACOLOGIA

Director de la Tesis:

Dr. Jorge Alberto Sánchez Rodríguez

Ciudad de México **Mayo, 2016**

CENTRO DE INVESTIGACIÓN Y DE ESTUDIOS AVANZADOS DEL INSTITUTO POLITÉCNICO NACIONAL

UNIDAD ZACATENCO

DEPARTAMENTO DE FARMACOLOGÍA

"Role of beta4 subunit of L-type calcium channels as a regulator of transcription in heart"

Eshwar Reddy Tammineni, M.Sc.

A Dissertation

Submitted in partial fulfilment of the

Requirements for the degree of

Doctor in Science

In the specialization of Pharmacology

THESIS DIRECTOR:

Dr. Jorge Alberto Sánchez Rodríguez

Mexico city **May, 2016**

Acknowledgement

Firstly, I would like to express my sincere gratitude to my advisor Dr. Jorge Alberto Sánchez Rodríguez, for the continuous support of my Ph.D. study and related research, for his patience, motivation, and immense knowledge. His guidance helped me in all the time of research and writing of this thesis. I could not have imagined having a better advisor and mentor for my Ph.D. study.

Besides my advisor, I would like to thank my thesis committee: Dr. Jose Antonio Terrón Sierra, Dra. Maria del Carmen García García, Dr. Carlos Martín Cerda García-Rojas, Dr. Sergio Sánchez-Armáss Acuña and Dr. Zurisaddai Hernández Gallegos, for their insightful comments and encouragement, but also for the hard question which incented me to widen my research from various perspectives.

I would like to Thank our lab auxiliary Dra. Elba Dolores Carrillo Valero for her technical assistance and continuous helpful discussions throughout my Ph.D. tenure without which this work would be far poorer. I would like to extend my sincere thanks to our lab auxiliary Ascensión Hernández Pérez (Tere) for technical support and knowledge. Thanks a lot Tere for always being so kind and caring for me.

My sincere thanks also goes to Dra. Maria del Carmen García García and Dra. Rosa Maria del Angel, who provided me an opportunity to access to their laboratory and research facilities. Without their precious guidance and support, it would not be possible to conduct this research. I would like to acknowledge Dr. Ruben Soto Acosta and Antonio H angel Ambrocio for numerous discussions and helping me to deal with virology part.

I would like to thank our lab technicians Oscar Ramírez Herrera and Lezama Sandoval Ivonne Yamilet for their assistance during experiments.

Many friends have helped me stay sane through these difficult years. Their support and care helped me overcome setbacks and stay focused on my graduate study. Gayathri,

Srikanth, Ateet, Selva, Tauqeer, Goldie, Vinoth, Ravichandran, and Rohini, Thanks, guys. We were not only able to support each other by deliberating over our problems and findings, but also happily by talking about things other than just our papers. It was always a friendly environment, and more comfortable worked together with all of you guys.

Most importantly, none of this would have been possible without the love and patience of my family. I would like to thank my parents, Mr. Shiva Reddy Tammineni and Mrs. Ramana Tammineni, my cousin Raja Shekar Reddy Peram and Madhuri Yeramala for all their appreciation all through my educational research career. Thank you for your encouragement, love and support.

Finally, I appreciate the financial aid from CONACyT who funded parts of the research discussed in this dissertation and supported with a scholarship for four years during my Doctorate in Science.

INDEX

Table of contents

Abbreviations

ADP - Adenosine diphosphate

AID - Alpha interacting domain

ATP - Adenosine triphosphate

BID - Beta interacting domain

CCAT - Calcium channel associated transcriptional regulator

DENV - Dengue virus

DHF - Dengue Hemorrhagic Fever

GMP - Guanosine monophosphate

GAS - Gamma-activated sequences

HVA - High-voltage-activated

IRFs - Interferon-regulatory factors

IFN - Interferon

ISREs - Interferon-stimulated response elements

IL - Interleukins

JAK - Janus kinase

LVA - Low voltage-activated

MAGUK - Membrane-associated guanylate kinases

MDA5 - Melanoma differentiation-associated gene 5

MOI - Multiplicity of infection

NS3 - Non-structural 3

NLRs - Node like receptors

PAGE - Polyacrylamide gel elctrophoresis

PRRs - Pattern recognition receptors

Poly (I:C) - Polyinosinic:polycytidylic acid

RIG-1 - Retinoic acid-inducible gene 1

RT-PCR - Real-time polymerase chain reaction

STAT - Signal transducer and activator of transcription

TLRs - Toll-like receptors

VGCC - Voltage-gated calcium channels

Figure Index

Table Index

Abstract

L-type voltage gated Ca^{2+} channels (VGCC) play a critical role in regulating electrical and biochemical pathways in cardiac muscle. They also regulate gene transcription by controlling Ca^{2+} influx. The principal subunit of VGCC is associated with β auxiliary subunits (β_1-β_4), which regulate channel gating properties. A novel role of the β_4 subunit has recently emerged in which it translocates to the nucleus and regulates gene transcription by interacting directly with nuclear proteins in cochlea and hippocampal neurons. Although β_4 subunit is expressed in heart, its direct involvement in regulating gene transcription has not been previously described.

Here we report the localization of β_4 subunit in nuclei of embryonic rat heart cells (H9c2) and that overexpression of β_4 subunit increases the expression of a wide variety of endogenous genes related to antiviral activity. This includes genes in the downstream signalling of RIG-1 pathway such as RIG-1 and Irf7. Interferon stimulating genes such as Ifitm3 were also upregulated. In agreement with these findings, we found upregulation of the corresponding antiviral proteins by β_4 subunit overexpression. Consistent with present findings, we observed that β_4 subunit has antiviral activity: to reach this conclusion we infected H9c2 cells with the dengue virus and found that dengue infection levels were greatly reduced in H9c2 cells that overexpressed β_4 subunit. We also found enhanced endogenous expression of β_4 subunit both at mRNA and protein levels in response to Dengue virus infection and most importantly, cells in proximity to virus infected cells showed a positive translocation of β_4 subunit to the nucleus. This suggests that a diffusible factor plays a role. In agreement with this possibility, we found that interferon treatment enhances expression of β_4 subunit, and inhibition of Jak Stat pathway using jak1 inhibitor GLPG0634 reduced the expression levels of β_4 subunit.

In conclusion, these findings provide evidence that in response to Dengue virus infection of H9c2 cells, β_4 subunit levels are increased. Infection also leads to β_4 subunit translocation to nucleus where it regulates gene transcription of antiviral genes and mediates cellular resistance to viral infection. The JAK-STAT pathway is possibly involved in these effects.

1. Introduction

1.1 L-Type calcium channels

Voltage-gated calcium channels (VGCC) are members of a superfamily of voltage-gated ion channels. VGCC are an important route of calcium entry into cardiac cells and are essential for converting electrical activity into biochemical reactions in excitable cells (Catterall et al., 2005). VGCC's are classified into high-voltage activated (HVA) and low-voltage activated (LVA) channels (Carbone & Lux, 1987). Later VGCC's are further classified into L, N, P/Q, R (HVA) and T (LVA) types based on their biophysical and pharmacological properties (Ellinor et al., 1993)(Table 1.1). Among these calcium channels, L-type calcium channels are critical in regulating calcium influx and further controls both excitation-contraction coupling and cardiac excitability. VGCC's are multimeric protein complexes consisting of four protein subunits: a principle pore forming α1 subunit and β, α2δ, γ auxiliary subunits which modulate trafficking and gating properties (Catterall, 2000) [Figure 1]. The α1 subunit is composed of 4 homologous domains (I–IV), each containing six transmembrane segments (S1–S6).

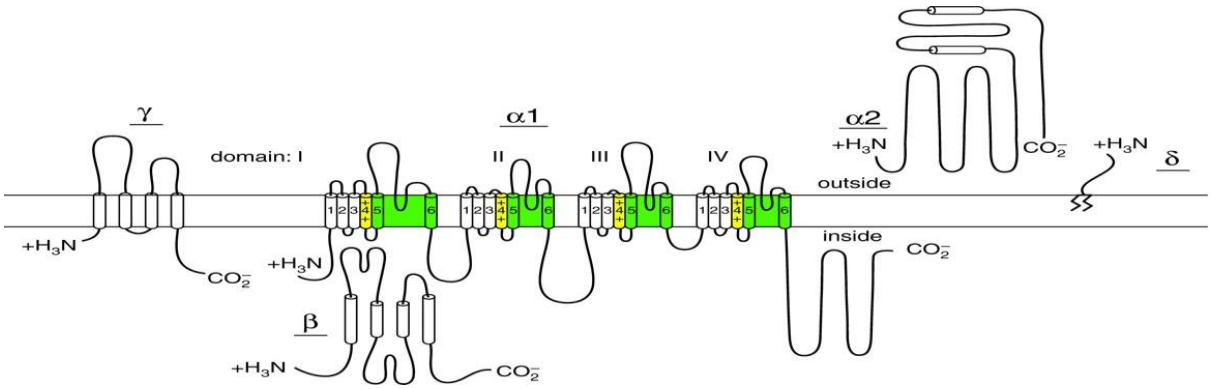

Figure 1.1: Schematic representation of VGCC showing the topology of the pore forming α1C subunit, and β, α2δ, γ auxiliary subunits (Catterall, 2000).

In cardiac muscle, L-type Ca^{2+} channels are primarily encoded by the α1C subunit ($Ca_v1.2$) and is involved in wide variety of physiological cardiac functions such as muscle contraction, hormone secretion, and gene expression with possible contribution by α1D as well ($Ca_v1.3$) (Mikami et al., 1989; Taylor et al., 2014). The pore-forming α1C subunit contains the voltage sensor and is the key component that determines the pharmacology and

channel identity, but its trafficking and functional properties are mainly regulated by auxiliary subunits.

Classification based on voltage	Biophysical classification	Molecular classification	Structural Nomenclature
High voltage activated channel (HVA)	L-type	α1S	$Ca_v1.1$
		α1C	$Ca_v1.2$
		α1D	$Ca_v1.3$
		α1F	$Ca_v1.4$
	P/Q type	α1A	$Ca_v2.1$
	N-type	α1B	$Ca_v2.2$
	R-type	α1E	$Ca_v2.3$
		α1G	$Ca_v3.1$
Low voltage-activated channel (LVA)	T type	α1H	$Ca_v3.2$
		α1I	$Ca_v3.3$

Table 1.1: Classification of voltage-gated calcium channels (Ellinor et al., 1993)

1.1.1 Auxiliary β subunit isoforms, expression and tissue distribution.

Principal α1 subunit is tightly bound to cytosolic β subunits having a molecular weight of 52 to 78 KDa coded by four Cacnb1-4 distinct genes. Each β subunit has its splice variants with different tissue distribution (Buraei & Yang, 2010) [Table 1.2]. Biochemical and primary sequence analyses indicate that the β subunits are hydrophilic in nature with no transmembrane segments. All four β subunits can dramatically enhance calcium channel currents when they are co-expressed in heterologous expression systems along with a Ca_v1 or Ca_v2 subunit.

β subunit	**Tissue distribution**
β_1	Expressed in the brain (cerebral cortex, habenula, hippocampus, and olfactory bulb), heart, skeletal muscle, spleen, and T cells, but not in kidney, liver, or stomach.
β_{1a}	Expressed exclusively in skeletal muscle
β_{1b}	Expressed in the brain (cerebellum and cerebral cortex), nerve endings at the neuromuscular junction and pancreas.
β_{1c}	Expressed in brain and spleen, but not in kidney, liver, muscle, or stomach
β_{1d}	Expressed in the heart.
β_2	Expressed in brain (hippocampus–becoming the most abundant isoform there, cerebellum, pontine nucleus, substantia nigra, central grey, habenula, pineal gland, thalamic nuclei, cerebrum), heart, lung, nerve endings at the NMJ, T cells, and osteoblasts, but not in kidney, liver, pancreas, or spleen.
β_{2a}	Expressed in brain, heart, and aorta.
β_{2b}	Expressed in brain, heart, and aorta. It is the most abundant β isoform expressed in human heart.
β_{2c}	Expressed in brain and heart.
$\beta_{2d,e}$	Expressed in the heart.
β_3	Expressed mostly in the brain (cerebellum, cerebral cortex, habenula, hippocampus, olfactory bulb, and striatum), but also in heart, aorta, kidney, lung, skeletal muscle, smooth muscle, spleen, thalamus, T cells, and trachea, but not in liver, pancreas, or testis.
$\beta_{3\ truncated}$	Expressed in brain, heart, and aorta.
β_4	Expressed in brain (cerebellum, brain stem, cerebral cortex, dentate gyrus, habenula, hippocampus, olfactory bulb, striatum, thalamus, and hypothalamus), kidney, nerve endings at the NMJ, ovary, skeletal muscle, spinal cord, T cells, and testis, heart, liver, lung, spleen, or thymus.
β_{4a}	Expressed in the spinal cord and cerebellum eye, heart and lung.
β_{4b}	Expressed in spinal cord, hippocampus, forebrain eye, lung and heart
β_{4c}	Expressed in the brain stem, cerebellum, eye heart and lung.
β_{4e}	Expressed in the brain cerebellum.

Table 1.2: Tissue distribution of β subunits (Buraei & Yang, 2010)

1.1.2 Structure of β subunits (members of MAGUK proteins)

Based on amino acid sequence alignment, biochemical and functional studies, and molecular modeling, it was found that β subunit is a modular structure consisting of five distinct regions. The first V1 is N-terminal region, third V3 is HOOK region , and fifth V5 is C-terminal region and is variable in length and amino acid sequence, whereas the second C2 and fourth C4 regions are highly conserved and are homologous to the Src homology 3 (SH3) and guanylate kinase (GK) domains, respectively (see Figure 1.3). The existence of an SH3-HOOK-GK module places β subunit in a family of proteins called Membrane-Associated Guanylate Kinases (MAGUKs).

Guanylate Kinases catalyze the formation of ADP and GDP from ATP and GMP. The general structural features of GK domain are well-preserved in the β subunit GK domain but structural variations exist in the catalytic site, and many key catalytic residues are absent in β subunit GK domain. Thus, GK domain of β subunit is catalytically inactive. Instead, β subunit GK domain has evolved into a protein interaction module, binding tightly to principal α1 subunit through its high-affinity interaction with the alpha interacting domain (AID).

All β subunits bind to the 18 amino acid AID in the I–II linker of Cav1 and Cav2 α1 subunits (Chen et al., 2004)(Figure 1.2). Single mutations of several conserved residues in the AID, including Y10, W13 and I14, significantly weaken the AID–Cavβ interaction in vitro and reduce or abolish Cavβ-induced stimulation of Ca^{2+} channel current in heterologous expression systems. A 31-amino acid segment of Cavβ, referred to as the β-interacting domain (BID), had been described as the main binding site for the AID. The BID was able to enhance slightly Ca^{2+} channel current and modulates gating (De Waard et al., 1994).

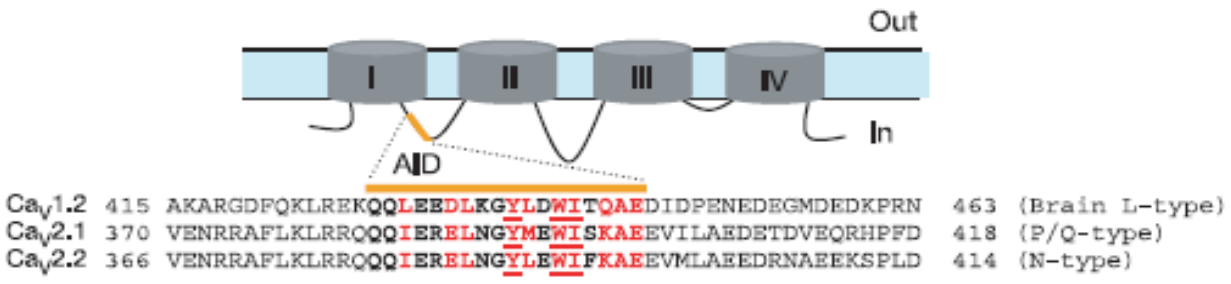

Figure 1.2: Alpha Interacting domain (AID). Residues forming the AID are in bold, and those involved in interactions with the β-subunit are in red, with the three most critical residues underlined (Chen et al., 2004).

In general, SH3 domains have a well conserved and compact fold consisting of five sequential β-strands assembled into two orthogonally packed sheets and are characterized by its interaction with particularly proline-rich motifs. They mediate specific protein-protein interactions by binding to PxxP-containing motifs in target proteins, through a surface formed by a cluster of highly conserved hydrophobic residues. The HOOK region is variable in length and amino acid sequence among the β subunit subfamilies. In the crystal structures, a large portion of the HOOK is unresolved due to poor electron density, indicating that it has a high degree of flexibility. The HOOK region plays a significant role in regulating channel inactivation.

The amino and carboxyl termini of β subunit are highly variable in length and amino acid composition. There is yet no structure available for β subunit C-terminus. However, an NMR structure of the NH2 terminus of β_4 subunit was solved recently, revealing a fold consisting of two α-helices and two antiparallel β- sheets (A. C. Vendel et al., 2006).

1.1.3 β_4 subunit isoforms, tissue distribution and subcellular localization

The β_4 subunit was cloned for the first time by Castellano et al. in 1993. So far, four splice variants of β_4 subunit have been identified (β_{4a}, β_{4b}, β_{4c}, β_{4e}) and β_{4b} was the first detected and it is a large size 519 amino acids isoform and molecular weight of 58 kDa. Helton and Horne in 2002 identified β_{4a} and it is shorter than β_{4b} and varies in the N-terminal region. β_{4c} subunit was first time identified by Hibino in 2003 and is similar to β_{4a}, lacking a complete C-terminal end. Solmaz Etemad et al. in 2014 discovered another N-terminal splice variant β_{4e} from mouse brain cerebellum (Figure1.3).

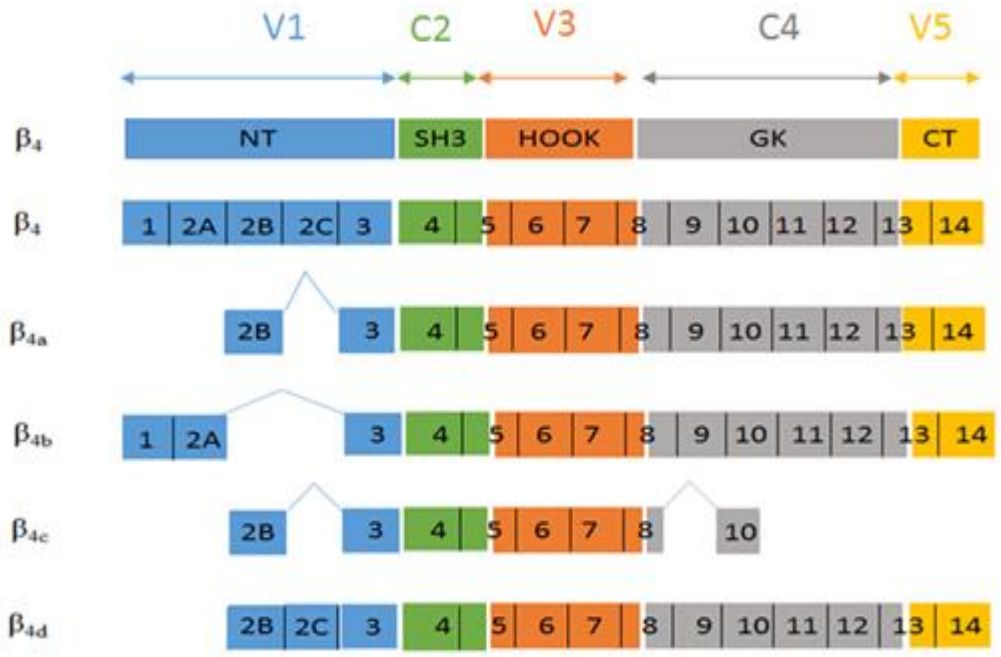

Figure 1.3: Different splice variants of β_4 subunit (Solmaz Etemad et al. 2014)

Thomas D. Helton et al. in 2002 reported a different pattern of distribution for β_{4a} and β_{4b} in the human central nervous system (CNS). β_{4a} was distributed throughout evolutionarily older regions of the CNS, β_{4b} was concentrated heavily in the forebrain (Helton et al., 2002). In the year 2006 Vendel et al. examined the expression of β_{4a} and β_{4b} in cerebellar cortex however immunohistochemistry experiments revealed that distribution of β_{4a} and β_{4b} are different. β_{4a} is expressed in the molecular layer, at the synapse level, in the cerebellum whereas β_{4b} is expressed in cell bodies of Purkinje cells and glia Bergmann (A. C. Vendel et al., 2006). In the same year, Colecraft et al. identified β_{4b} subunit in the nucleus of rat cardiomyocytes when they exogenously over expressed GFP-tagged β_{4b} using adenoviral vectors (Colecraft et al., 2002). On the other hand, Foel et al. in 2004 reported the endogenous expression of β_{4b} in canine cardiomyocytes with preferential distribution in surface sarcolemma (J. D. Foell et al., 2004). Other studies shown that β_{4b} was identified in the cerebellar cortex and the deep cerebellar nuclei regions subcellular studies demonstrated that β_{4b} was concentrated in the nuclei of Purkinje cells and granule cells (Subramanyam et al., 2009).

A new splice variant β_{4c} was discovered in chicken by Hibino et al. in 2003. β_{4c} splice variant corresponds to truncated form of β_{4a} subunit. Its tissue distribution was analyzed using RT-PCR, and they found that β_{4c} in the brain, spinal cord spinal, eyes and heart. Subcellular localization studies revealed that β_{4c} was identified in the nucleus of tsA201 cells when they overexpressed with GFP-tagged β_{4c} (Hibino et al., 2003). More recently, the same

group has detected β_{4c} in the human brain and the vestibular nuclei of neurons (Xu et al., 2011).

Recently in 2014, Solmaz Etemad et al. identified a new splice variant β_{4e}, which is lacking N-terminus and is highly expressed in mouse cerebellum and cultured cerebellar granule cells. Compared with the other two known full-length β_4 subunit variants (β_{4a} and β_{4b}), the β_{4e} subunit is most abundantly expressed in the distal axon but lacks nuclear-targeting properties (Etemad et al., 2014).

1.1.4 Voltage-gated calcium channels in regulating gene transcription

Calcium acts as a second messenger, and it has been implicated in a variety of biological functions such as proliferation, protein synthesis, and differentiation, but it also engaged in more specific cell functions like muscle contraction, neurotransmitter release, electrical excitability, and synaptic plasticity. Calcium levels are relatively high in the extracellular space (1 to 2 mM). A strict spatiotemporal control of the intracellular concentration of Ca^{2+} is required to allow this second messenger to get involved in a wide variety of cell functions. Ca^{2+} homeostasis is regulated by different channels, localized both at the plasma membrane and intracellular organelles that permit elevation of cytosolic calcium. VGCC are one of such channels that are localized in the plasma membrane and control the entry of Ca^{2+} into the cell. In general, three different signalling pathways link VGCC and gene expression have been described.

The first pathway involves VGCC that control the entry of calcium into the cell and regulate the activity of cytoplasmic calcium-binding proteins that propagate the information to the nucleus and modify gene transcription. Morgan JI et al. in the year 1986 delivered first such evidence and found that chronic depolarization of pheochromocytoma (PC12) cells induces an increase in c-fos expression levels. This effect was blocked by nisoldipine, an L-type channel inhibitor, as well as by trifluoroperazine or chlorpromazine, two antagonists of calmodulin. It was therefore concluded that cytoplasmic Ca^{2+} elevation driven by L-type calcium channels turns on a calmodulin-dependent expression of c-fos (Morgan & Curran, 1986). This study pointed out that this entry pathway of Ca^{2+} is relevant for the gene regulation and activation of particular genes.

The second pathway involves VGCC controlling the calcium influx that directly moves to the nucleus, where it interacts with proteins related to gene transcription. Two modes of nuclear accumulation of Ca^{2+} have been explained. On the one hand, Ca^{2+} from L-type channels activate surrounding calmodulin that then translocates and accumulates in the nucleus (Mermelstein et al., 2001). Nuclear calmodulin plays a role in the activation of nuclear proteins such as CaMK. On the other hand, Ca^{2+} entry following electrical activation induces Ca^{2+} release from internal stores allowing propagation of the Ca^{2+} signal from the periphery of the cell to the nucleus. In both cases, VGCC control the influx of calcium which further enters the nucleus and regulates gene transcription by binding to calcium binding proteins.

In striking contrast to these two routes, the third pathway involves an entirely new concept of VGCC function where calcium channel domains act as transcription factors. Indeed, it was demonstrated that domains of VGCC, either a complete subunit or a fragment of a subunit directly relocate to the nucleus under certain circumstances and directly participate in gene regulation. The very first evidence that this might be the case came from a study of Hibino and collaborators in 2003 (Hibino et al., 2003). In this work, the authors demonstrated that a short particular splice variant of β_4, termed β_{4c}, interacts with heterochromatin protein 1γ (CHCB2/HP1γ), a nuclear protein involved in gene silencing and transcriptional regulation (Eissenberg et al., 1990). The interaction between β_{4c} and CHCB2/HP1γ is required for nuclear translocation of $\beta_{4c,}$ and furthermore, β_{4c} dramatically reduced the gene silencing activity of heterochromatin protein 1γ (Hibino et al., 2003).
In a separate study it was demonstrated that a proteolytic fragment of the C-terminus of the pore-forming subunit of L-type channels (Ca_v 1.2) encodes a transcription factor (Gomez-Ospina et al., 2006). This domain is called calcium channel associated transcriptional regulator (CCAT). Using antibodies that recognize C-terminus of Ca 1.2, the authors demonstrated the occurrence of CCAT in the nucleus of neurons from developing and adult brains. The transfer of CCAT out of the nucleus is activated by an increase in intracellular Ca^{2+} resulting from L-type calcium channel opening. CCAT was found allied with p54(nrb)/NonO, a nuclear protein that plays a role in changing the transcription downstream of the neuronal Wiscott Aldrich Protein. Using oligonucleotide microarray, they recognised many genes that are down- or up-regulated by CCAT. Among the regulated genes (using luciferase reporter assays) they showed that CCAT enhanced the promoter activity of Cx31.1 gene.

Recently in 2015, Ling Lu et al. reported that the C-terminus of $Ca_v1.3$ translocates to the nucleus of atrial myocytes where it functions as a transcriptional regulator to modulate the function of Ca^{2+} activated potassium channels (Lu et al., 2015). Intracellular Ca^{2+} directly regulates nuclear translocation of the C-terminal domain of Cav1.3. By using a *Cav1.3* null mutant mouse model, they demonstrated that knockout of $Ca_v1.3$ results in a reduced protein expression of myosin light chain 2, which interacts with and increases the membrane localization of Ca^{2+} activated potassium channels.

1.1.5 Auxiliary β subunits directly involved in regulating gene transcription.

The β subunits are involved in several functions such as trafficking of principle α1 subunit to the plasma membrane, promoting VGCC gating resulting in an overall enhancement of current. The β subunits interact with the ryanodine receptor in the sarcoplasmic reticulum of muscle cells and is critical for excitation–contraction coupling. β subunits interact directly with many intracellular proteins that regulate VGCC function. In recent times, it has become evident that these complete VGCC β subunits relocate to the nucleus under certain circumstances and are directly involved in gene regulation (Buraei & Yang, 2013)(Figure1.4).

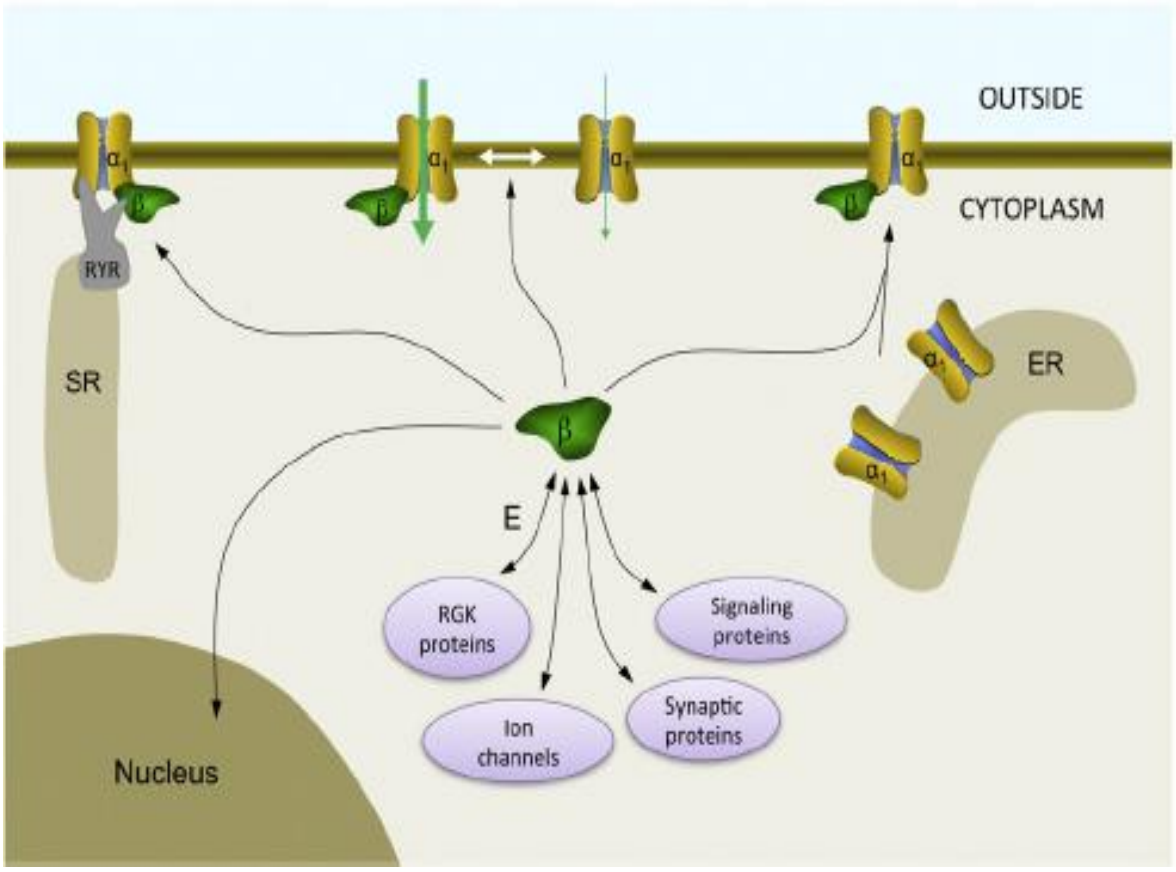

Figure 1.4: Major functions of β subunits (Buraei & Yang, 2013).

Jackson Taylor and co-authors in 2014 reported the localization of β_{1a} subunit in the nucleus of proliferating muscle progenitor cells (MPC) under both endogenous and overexpressed condition. Loss of β_{1a} expression impaired MPC expansion in vitro and in vivo and caused widespread changes in global gene expression, including up-regulation of myogenin (Taylor et al., 2014). They also found that β_{1a} subunit localizes to the promoter region of some genes, preferentially at non-canonical (NC) E-box sites. β_{1a} subunit binds to a region of the myogenin promoter containing an NC E-box, suggesting a mechanism for inhibition of myogenin gene expression. Similar observations were made on another β subunit as well. Yun Zhang et al. in 2009 reported that β_3 subunit was translocated into the nucleus of HEK 293T cells when they co-transfected with Pax6(S), splicing isoform of a transcription factor that belongs to the paired box (Pax) family (Pax6) (Zhang et al., 2010) in addition, using luciferase reporter assays they found that β_3 subunit is able to suppress the transcriptional activity of Pax6(S) by 50%.

Hibino et al. in 2003 reported nuclear localization and transcriptional activity of truncated form of β_4 subunit (β_{4c}). However nuclear localization of complete β_4 subunit came into focus only when two independent studies reported the localization of β_{4b} subunit in adult rat cardiomyocytes (Colecraft et al., 2002) and hippocampal neurons (Subramanyam et al., 2009). Tadmouri et al. in 2012 studied the nuclear function of β_{4b} subunit and reported its involvement in transcriptional activity in hippocampal neurons (Tadmouri et al., 2012).

β_{4b} subunit translocation from the cytoplasm to the nucleus is observed during neuronal differentiation. This translocation depends on β_{4b} structural integrity and more precisely on the interaction between the β_{4b} SH3 (Src Homology 3) and GK (Guanylate Kinase) domains. β_4 nuclear translocation is conditioned by its association with a partner: the regulatory subunit of phosphatase protein 2A (PP2A), B56δ. Membrane depolarization induces β_4 channel uncoupling and association with B56δ. Thus, β_4 migrates to the nucleus forming a complex with B56δ/PP2A. A further study on gene expression analysis generated by microarray studies comparing profiles of lethargic mice, considered as spontaneous β_4 knockout with wild-type mice cerebellum was done. This study described the influence of β_4 on the repression and the activation of certain genes. Particularly, β_4 strongly repressed tyrosine hydroxylase (TH) gene expression. In the nucleus, β_4 interacts with a transcription factor: the thyroid hormone receptor. This association allows β_4/B56δ/PP2A complex to target the TH gene promoter (Tadmouri et al., 2012).

Subcellular distribution of β_4 subunit in cardiomyocytes remains controversial. Colecraft et al. in 2002 demonstrated the significant distribution of β_4 subunit in the nucleus of adult rat cardiomyocytes when they overexpressed with GFP-tagged β_4 subunit using adenoviral vectors (Colecraft et al., 2002). On another hand in 2004, Foell and their group reported the endogenous expression of β_4 subunit restricted to the plasma membrane in canine cardiomyocytes (Jason D Foell et al., 2004).

The characterization of the subcellular localization of β_4 subunit in heart cells and its possible role in functions other than modulating Ca^{2+} channel currents is therefore of significant scientific relevance.

1.2 Innate immunity

Innate immunity is characterized by the presence of Germline-encoded pattern recognition receptors (PRRs) which sense components specific to microorganisms (Medzhitov et al., 2007). Recent studies have identified four major classes of PRRs responsible for sensing foreign material. They are designated as Toll-like receptors (TLRs), retinoic acid-inducible gene I (RIG-I)-like helicases (RLHs), C-type lectin receptors (CLRs) and nucleotide oligomerization domain (NOD)-like receptors (NLRs) (table 1.3) (Takeuchi & Akira, 2010). These PRRs are expressed not only in immune cells such as macrophages and dendritic cells but also in various nonprofessional immune cells. During viral infections, the virus will secrete its genetic material into a host system to propagate its number. TLRs and RLHs recognize viral genetic material such as RNA and DNA, and cells are activated to produce type I interferons (IFNs) and proinflammatory cytokines. Type I IFNs, comprised of multiple IFN-α isoforms, a single IFN-β, and other members, such as IFN-ω, IFN-ε and IFN-κ, are pleiotropic cytokines that are essential for antiviral immune responses (Honda et al., 2006). These interferons induce apoptosis of virus-infected cells through different mechanisms and provide cellular resistance to virus infection.

1.2.1 Different types of pattern recognition receptors (PRR's)

1.2.1.1 Toll-like receptors (TLRs)

TLRs are responsible for sensing invading pathogens outside the cell and in intracellular endosomes and lysosomes (Takeuchi & Akira, 2010). TLRs comprised of the leucine-rich repeats (LRRs), a transmembrane domain, and a cytoplasmic Toll/interleukin 1 receptor (IL-1R) homology (TIR) domain (Akira et al., 2006). Until now, ten TLRs have been identified in humans and twelve in mice (Table 1.3). TLR2 forms heterodimers either with TLR1 or TLR6 to recognize distinct ligands (triacyl and diacyl lipoproteins). These triacyl and diacyl lipoproteins induce the production of different types of pro-inflammatory cytokines based on cell types involved (Barbalat, Lau, Locksley, & Barton, 2009). TLR4 recognizes lipopolysaccharide (LPS) together with myeloid differentiation factor 2 (MD2) on the cell surface where LPS is a component derived from the outer membrane of Gram-negative bacteria (Takeuchi & Akira, 2010). TLR4 is also involved in the recognition of viruses by binding to viral envelope proteins. TLR5 is highly expressed by DCs of the lamina propria

(LPDCs) in the small intestine, where it recognizes flagellin from flagellated bacteria. TLR11, which is present in mice but not in humans, detects uropathogenic bacteria (Yarovinsky et al., 2005). TLR3, TLR7, TLR8 and TLR9 are involved in the recognition of viral and bacterial nucleotides. TLR3 recognize double-stranded (ds) RNA while TLR7 and TLR8 detect single-stranded (ss) RNA and TLR9 recognizes unmethylated DNA with CpG motifs. TLR-mediated signaling pathways recruit TIR domain-containing adaptors such as MyD88 and TIR domain-containing adaptor inducing IFN-b (TRIF), thereby leading to activation of transcription factors such as nuclear factor-kB (NF-kB) and IFN-regulatory factors (IRFs), which regulate the expression of genes that encode proinflammatory cytokines and type I IFNs, respectively (Takeuchi & Akira, 2009). Since TLRs are transmembrane proteins, they are not able to detect viral components present in the cytoplasm of a cell.

PRRs	Localization	Ligand	Origin of the Ligand
TLR			
TLR1	Plasma membrane	Triacyl lipoprotein	Bacteria
TLR2	Plasma membrane	Lipoprotein	Bacteria, viruses, parasites, self
TLR3	Endolysosome	dsRNA	Virus
TLR4	Plasma membrane	LPS	Bacteria, viruses, self
TLR5	Plasma membrane	Flagellin	Bacteria
TLR6	Plasma membrane	Diacyl lipoprotein	Bacteria, viruses
TLR7 (human TLR8)	Endolysosome	ssRNA	Virus, bacteria,
TLR9	Endolysosome	CpG-DNA	Virus, bacteria, protozoa, self
TLR10	Endolysosome	Unknown	Unknown
TLR11	Plasma membrane	Profilin-like molecule	Protozoa
RLR			
RIG-I	Cytoplasm	Short dsRNA, 5'triphosphate dsRNA	RNA viruses, DNA virus
MDA5	Cytoplasm	Long dsRNA	RNA viruses
LGP2	Cytoplasm	Unknown	RNA viruses
NLR			
NOD1	Cytoplasm	iE-DAP	Bacteria
NOD2	Cytoplasm	MDP	Bacteria
CLR			
Dectin-1	Plasma membrane	b-Glucan	Fungi
Dectin-2	Plasma membrane	b-Glucan	Fungi
MINCLE	Plasma membrane	SAP130	Self, fungi

Table 1.3: PRRs and Their Ligands (Takeuchi & Akira, 2010).

1.2.1.2 RIG-I-like receptor (RLR) family and virus recognition

RLR family is comprised of three key proteins that include retinoic acid-inducible gene **1** (RIG-I; also known as DDX58), melanoma differentiation-associated gene 5 (MDA5; also known as helicard or IFIH1) and LGP2 (also known as dhx58) (Takeuchi & Akira, 2009). RLRs are comprised of two N-terminal caspase-recruitment domains (CARDs), a central DEAD box helicase/ATPase domain, and a C-terminal regulatory domain. RIG-I was identified as a candidate of a cytoplasmic viral genomic RNA detector. RLHs interact with dsRNAs through their helicase domain, and dsRNA stimulation induces their ATP catalytic activity. A C-terminal portion of RIG-I, designated the repressor domain (RD), was shown to inhibit the triggering of RIG-I signaling in the steady state, and the N-terminal CARDs handle activating downstream signalling pathways that mediate dsRNA-induced type I IFN production (Yoneyama et al., 2004). IFNs strongly induce the expression of genes encoding RLHs.

The CARDs of RIG-I and MDA5 induces signalling cascades. RIG-I and MDA5 associate with an adaptor protein, IFN-b promoter stimulator1 (IPS-1; also known as MAVS) localized in the mitochondrial outer membrane (Kawai et al., 2005; Seth et al., 2005). IPS-1 was found to associate with TNF-receptor-associated factor (TRAF) 3, an E3 ubiquitin ligase assembling lysine 63-linked polyubiquitin chains, through its C-terminal TRAF domain (Saha et al., 2006). TRAF3 recruits and activates two IKK-related kinases, designated TANK-binding kinase 1 (TBK1) and inducible IkB kinase (IKK-i; also known as IKKe), which phosphorylate IRF-3 and IRF-7 (Fitzgerald et al., 2003; Sharma et al., 2003). Phosphorylation of IRF-3 and IRF-7 by these kinases induces the formation of homodimers and/or heterodimers (Honda et al., 2005), which translocate to the nucleus and bind to IFN- (ISREs), resulting in the expression of type I IFN genes and a set of IFN-stimulated genes.

1.2.1.3 NLR- and CLR-Mediated Pathogen Recognition

The NLR family consists of cytoplasmic pathogen sensors that are composed of a central nucleotide-binding domain and C-terminal leucine-rich repeats. The N-terminal portions of most NLRs harbor protein-binding motifs, such as CARDs. NOD1 and NOD2 induce transcriptional upregulation of proinflammatory cytokine genes. NOD1 and NOD2 recognize the structures of bacterial peptidoglycans, g-D-glutamyl-mesodiaminopimelic

acid (iE-DAP) and muramyl dipeptide (MDP), respectively. CLRs comprise a transmembrane receptor family characterized by the presence of a carbohydrate-binding domain. CLRs recognize carbohydrates on microorganisms such as viruses, bacteria, and fungi. CLRs either stimulate the production of proinflammatory cytokines or inhibit TLR-mediated immune complexes.

1.2.2 Interferon signalling pathway

Once viral infection has taken place, different pattern recognition receptor pathways stimulate the expression of cytokines. Interferons are one among many cytokines that are soluble in nature. There are two independent types of interferon pathways. Type I interferon pathway includes IFNα, IFNβ and many more variants, whereas type II interferon has only one variant, i.e., IFNγ.

During type I interferon signalling, corresponding interferons (mainly IFNα, IFNβ) will engage with the interferon-α receptor (IFNAR, which is composed of the IFNAR1 and IFNAR2 subunits) activating Janus kinase 1 (JAK1) and tyrosine kinase 2 (TYK2). Phosphorylation of the receptor by these kinases results in the recruitment of signal transducer and activator of transcription (STAT) proteins, phosphorylation, dimerization and nuclear translocation. The three main STAT complexes that are formed in response to type I interferon (IFN) control distinct gene-expression programmes. The interferon-stimulated gene factor 3 (ISGF3) complex (which is composed of STAT1, STAT2 and IFN-regulatory factor 9 (IRF9)) binds to IFN-stimulated response element (ISRE) sequences leading to activation of classical antiviral genes, whereas STAT1 homodimers bind to gamma-activated sequences (GASs) and induces pro-inflammatory genes (Figure 1.5). In the type II IFN pathway, IFN-γ binds to a distinct cell-surface receptor, which is known as the type II IFN receptor. This receptor is also composed of two subunits, IFNGR1 and IFNGR2, which are associated with JAK1 and JAK2, respectively. Activation of the JAKs that are associated with the type II IFN receptor results in phosphorylation of STAT1 which induce the formation of STAT1–STAT1 homodimers that translocate to the nucleus and binds to GAS (IFN-γ-activated site) elements that are present in the promoter of certain interferon stimulated genes, thereby initiating the transcription of these genes.

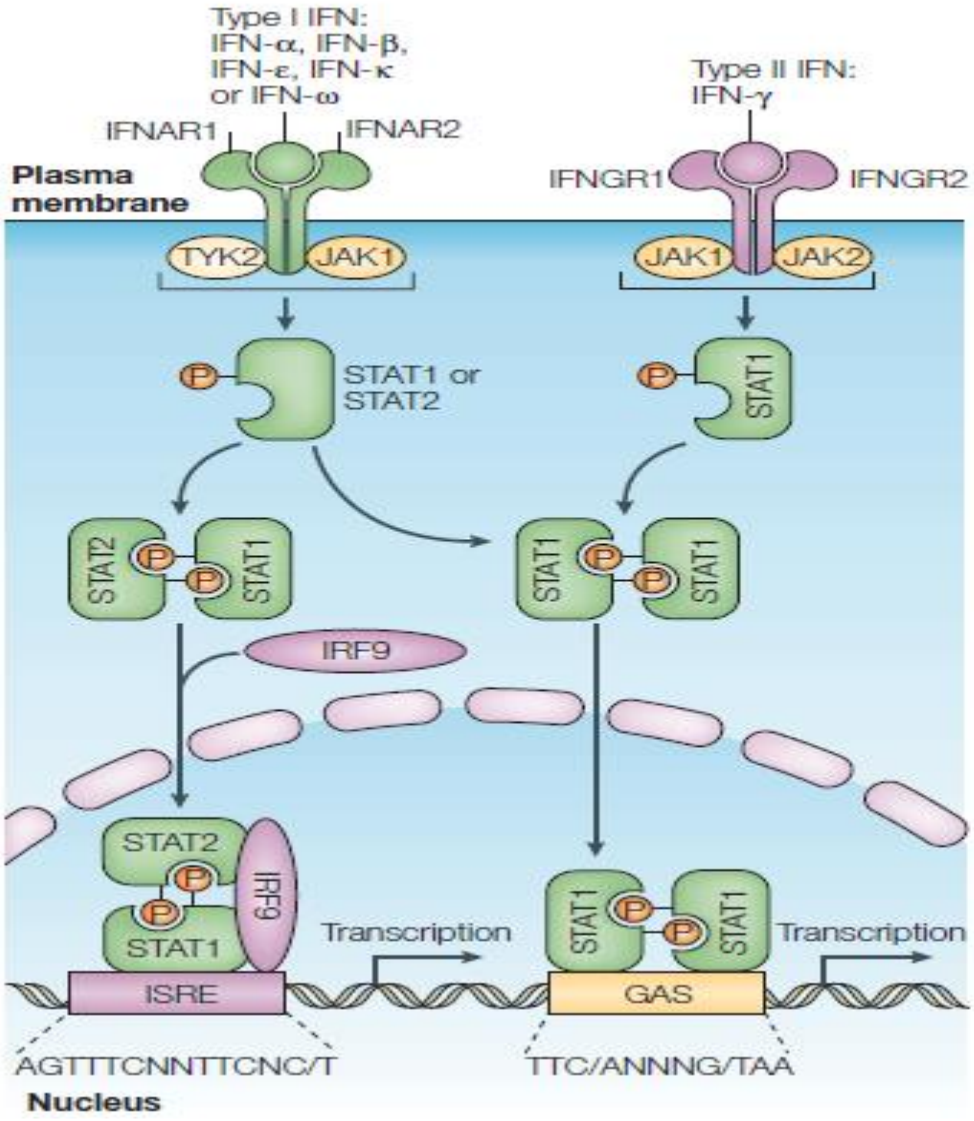

Figure 1.5: Interferon JAK-STAT pathway (Platanias, 2005).

1.2.3 Voltage-gated calcium channels regulating immunity.

The effects of VGCC on immune signalling pathways have been studied in immune cells. Burgess et al. reported that elevation of intracellular free Ca^{2+} ($[Ca^{2+}]i$) is an essential triggering signal for T cell activation by antigen and other stimuli that cross-link the T cell antigen receptor (TCR). Besides the involvement of calcium channels in regulating calcium influx, which in turn triggers T cell activation, VGCC subunits are also directly involved in controlling immune signalling events. Thus, It has been demonstrated that ataxia and seizures in the lethargic mouse arise from a mutation of the β_4 subunit gene (Burgess et al.,

1997). Interestingly, these mice experience an immunological disorder, including a defect in their cell-mediated immune response (Morrison 1984). At the beginning, the mechanism involved in the immune disorder shown in these lethargic β_4 mutant mice was not understood. Later on, Abdallah Badou et al. demonstrated that CD4+ T cells deficient in either β_3 or β_4 exhibit impaired NFAT activation, cytokine interferon γ production along with reduced Ca^{2+} response (Badou et al., 2006). Interestingly, in β_4-deficient T cells, a notable and specific suppression of the Cav1.1 pore-forming α1 subunit protein was described (Badou et al., 2006).

In CD8+ T cells, β_3 is highly expressed in naïve activated CD8+ T cells, and β_3 deficiency leads to enhanced apoptosis of naïve T cells and decrease the survival of these cells (Jha et al., 2009). Impaired Ca^{2+} influx in β_3-deficient CD8+ T cells was associated with a lack of Cav1.4 protein expression (Jha et al., 2009). These observations suggest that impairment of signalling events that took place in β_4 or β_3 deficient T cells might be due to reduced expression of the Cav1 channel. However, the exact mechanism and the requirement of multiple β regulatory subunits in effector T cell stage is still not clear. Two other L-type Ca^{2+} channels, CaV1.2 and CaV1.3, may play a role in Th2 cells, given that their depletion by RNAi impaired TCR-induced Ca^{2+} influx and IL-4 production in vitro and reduced airway inflammation in a passive transfer mouse model of allergic asthma (Cabral et al., 2010). CaV1.4 deficient mice also failed to mount an effective antigen-specific CD8+ T cell response to Listeria monocytogenes (Omilusik et al., 2011).

It was also reported that during different viral infections, expression of VGCC subunits was altered in diverse in-vitro and in vivo models. On the other hand targeting VGCC subunits reduced viral infection levels. Theiler's murine encephalomyelitis virus infected astrocytes revealed the upregulation of both VGCC Cav1.2 and Cav2.2 subunits along with Ca2+ currents with a density proportional to the amount of viral particles used for infection (Rubio et al., 2013). Knockdown of VGCC subunits such as β_3 and α1S reduced infection levels of mouse mammary tumor virus and Junín virus–cell in U2OS cells (Lavanya et al., 2013). On other hand injection of gabapentin into mice that specifically targets α2δ2 subunit diminished Junín virus–cell fusion and entry into cells and thereby decreased infection levels of Junín virus (Lavanya et al., 2013).

1.3 Dengue virus

1.3.1 Dengue viral infections

Dengue is the most significant arthropod-borne viral infection of humans. Worldwide, an estimated 2.5 billion people are at risk of infection, around 975 million of whom live in urban areas in tropical and sub-tropical countries in Southeast Asia, the Pacific and the Americas (Guzmán & Kouri, 2002). It is estimated that more than 50 million infections occur each year, including 500,000 hospitalizations for dengue hemorrhagic fever (DHF), mainly among children, with the case fatality rate exceeding 5% in some areas (Gubler, 2004; Guzmán & Kouri, 2002). DHF first emerged as a public health problem in 1954, when the first epidemic occurred in Manila. This gradually spread to other countries in the region. Major epidemics occurred in other areas of the world in the 1980s and 1990s and were caused by all four dengue viral serotypes (Nimmannitya 2002). The average annual number of dengue fever/dengue haemorrhagic fever (DF/DHF) cases reported to the World Health Organization (WHO) has increased dramatically in last few years. For the period 2000–2004, the annual average was 925,896 cases, almost double the figure of 479,848 cases that was reported for the period 1990–1999. In 2001, a record 69 countries reported dengue activity to WHO and in 2002, the region of the Americas alone reported more than 1 million cases (Gubler, 2004; Guzmán & Kouri, 2002). Travellers from endemic areas might serve as vehicles for further spread (Miller et al., 2007).

1.3.2 Clinical manifestations of dengue infections

Dengue infections may be asymptomatic or give rise to undifferentiated fever, dengue fever, DHF, or dengue shock syndrome. Undifferentiated fever usually follows a primary infection but may also occur during a secondary infection. Clinically it is indistinguishable from other viral infections.

Dengue fever may occur either during primary or secondary infections. The onset is sudden with high fever, severe headache (especially in the retro-orbital area), arthralgia, myalgia, anorexia, abdominal discomfort, and sometimes a macular papular rash. The fever may be biphasic and tends to last for 2–7 days (Farid et al., 2001). Flushing, a characteristic feature is commonly observed on the face, neck, and chest. Coryza may also be a prominent

symptom especially in infants (Hongsiriwon, 2002). Younger children tend to present with coryza, diarrhea, rash and seizure, and less commonly with vomiting, headache, and abdominal pain. Although, haemorrhagic manifestations are uncommon in dengue fever, gastrointestinal bleeding, epistaxis, and gingival bleeding have been observed in some individuals (S K Kabra et al., 1992). A positive tourniquet test has been reported in many individuals with dengue fever possibly due to reduced capillary fragility (Kalayanarooj S & Nimmannitya S, 1999). Recovery from dengue fever is usually uneventful, but may be prolonged especially in adults.

DHF usually follows secondary dengue infections, but may sometimes follow primary infections, especially in newborns. Such a phenomenon has not been described in human infections other than dengue. DHF is characterised by high fever, haemorrhagic phenomena, and features of circulatory failure. For purposes of description, DHF is divided into three phases, they are febrile, leakage, and convalescent phases. Furthermore, according to severity DHF is divided into four grades.

Grade I: no shock: only positive tourniquet test.

Grade II: no shock; has spontaneous bleeding other than a positive tourniquet test.

Grade III: shock.

Grade IV: profound shock with intense blood pressure or/and pulse.

In DHF, bleeding may occur from any site and does not correlate with the platelet counts. Haemorrhagic manifestations usually occur once the fever has settled (Richards et al., 1997). Minor degrees of bleeding may manifest as gum bleeding and petechiae. The commonest site of haemorrhage is the gastrointestinal tract, which displays as haematemesis or melaena, followed by epistaxis. Vaginal bleeding is commonly reported in females (Guzman et al., 1984).

Dengue shock syndrome is associated with very high mortality (around 9.3%, increasing to 47% in instances of profound shock) (Kabra et al., 1999). Severe plasma leakage results in dengue shock syndrome, with symptoms of cold blotchy skin, circumoral cyanosis, and circulatory disturbances. Acute abdominal pain and persisting vomiting are early warning signs of impeding shock (Guzmán et al., 1999). Sudden hypotension may indicate the onset of profound shock (Agarwal et al., 1999). Prolonged shock is often accompanied by metabolic acidosis, which may precipitate disseminated intravascular coagulation or enhance ongoing disseminated intravascular coagulation, which in turn could lead to

massive haemorrhage. Encephalopathy may accompany dengue shock syndrome due to metabolic or electrolyte disturbances.

1.3.3 Characteristics of dengue virus

The dengue virus is a single-stranded RNA virus belonging to the Flaviviridae family (Guzmán & Kouri, 2002). There are four serotypes (DEN 1–4), classified based on biological and immunological criteria. The viral genome is approximately 11 kb in length (Guzmán & Kouri, 2002). The mature virion consists of three structural (core, membrane associated, and envelope) and seven non-structural (NS1, NS2a, NS2b, NS3, NS4a, NS4b, and NS5) proteins. The envelope protein is involved in the main biological functions of the virus. It binds to receptors on host cells, allowing the virus to be transported through it. Also, the envelope protein is associated with haemagglutination of erythrocytes, induction of neutralising antibodies and protective immune responses (M G Guzmán & Kourí, 1996).

Non-structural proteins (NS1–NS5) expressed as both membrane-associated and secreted forms have also been implicated in the pathogenesis of severe disease. Unlike other viral glycoproteins, NS1 does not form a part of the virion but gets expressed on the surface of infected cells. Preliminary evidence suggests its involvement in viral RNA replication (Young et al., 2000). Plasma levels of secreted NS1 (sNS1) correlate with viral titres, being higher in patients with DHF compared with dengue fever (Libraty et al., 2002).

1.3.4 Cytokine responses in dengue infections

Dengue virus infected monocytes, B-lymphocytes, and mast cells produce different cytokines. At present, there is disagreement about the predominant cytokines produced during dengue fever and DHF. According to Chaturvedi et al., serum concentrations of tumour necrosis factor-a (TNF-a), interleukin (IL)-2, IL-6, and IFN-γ are highest in the first three days of illness whereas IL-10, IL-5, and IL-4 tend to appear later (Chaturvedi et al., 1999). IL-2 and IFN-γ are Th1 and IL-5 and IL-4 Th2 type cytokines. Thus, it has been suggested that Th1 responses are seen during the first three days, and Th2 responses occur later (Chaturvedi et al., 1999). Increased levels of IL-13 and IL-18 have also been reported during severe dengue infections, with highest levels seen in patients with grade IV DHF. Serum IL-12 levels are highest in patients with dengue fever but undetectable in patients

with grade III and IV DHF. DHF patients have higher levels of TNF-a, IL-6, IL-13, IL- 18, and cytotoxic factor compared with DF patients. These cytokines have been implicated in causing increased vascular permeability and shock during dengue infections (Mustafa et al., 2001). Moreover, cytotoxic factor, produced by CD4+ T-cells, induces macrophages to produce the proinflammatory cytokines IL- 1a, TNF-a, and IL-8. Levels of cytotoxic factor correlate with disease severity (being highest in patients with grade IV DHF).

1.3.5 Dengue infection in heart

Dengue targets different tissues in human body. It has been identified that different immune cells such as resident cutaneous Langerhans dendritic cells, monocytes, macrophages, as well as B and T cells have been characterized as the primary targets of the viral infection in humans and in mice in vivo. However, in recent years, it has been described typical clinical symptoms in dengue patients, involving the lung, kidney, central nervous system and heart. Injuries in these organs have been confirmed by hemorrhage, edema and inflammatory infiltrate.

Cardiac involvement in dengue has been reported in few studies, usually resulting in a benign and self-limited disease. Reports of more severe disease with progression to cardiogenic shock and death has also been described (Obeyesekere & Hermon, 1973). In an evaluation of 17 dengue patients with radionuclide ventriculography, Wali et al., showed that 7 patients had an ejection fraction of <40% and 12 had global hypokinesia, and that, after 3 weeks of follow-up, all alterations had returned to normal (Wali et al., 1998). In another report of 102 children with DHF, ten patients had acute myocarditis requiring the use of inotropic drugs due to acute heart failure(Salgado et al., 2009). Several studies have reported myocardial dysfunction in acute dengue using different techniques (Table 1.4)

The mechanism of myocardial damage in dengue could be the release of inflammatory mediators and/or the direct action of the virus on cardiomyocytes as seen in acute myocarditis caused by other viruses (Leslie T. Cooper, 2009). The possible mechanisms involved in cardiac manifestations of dengue comprise functional myocardial impairment, arrhythmias, and myocarditis are shown in the figure 1.6.

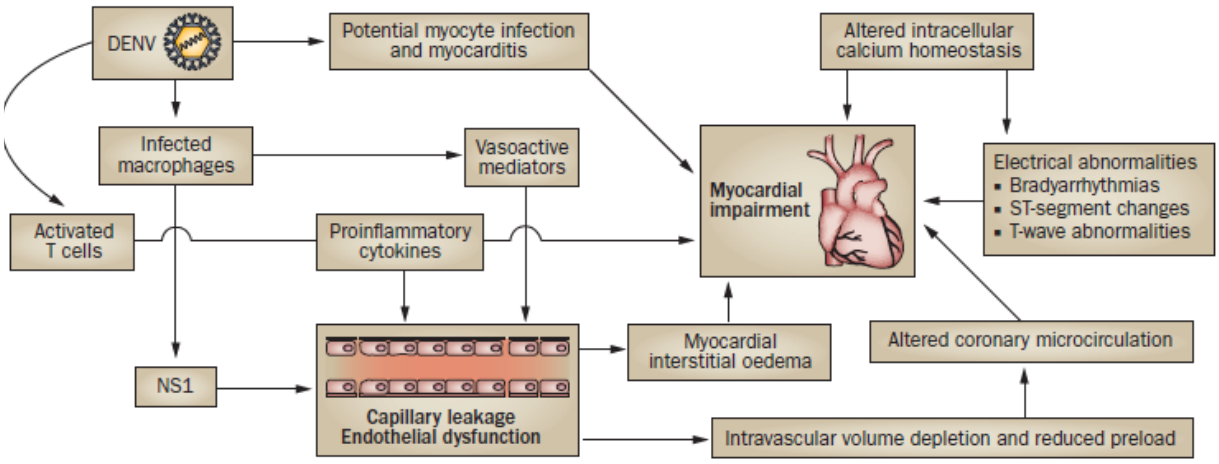

Figure 1.6: Proposed viral and immune mechanisms involved in the cardiac and vascular manifestations of dengue. DENV is taken up into macrophages with the resulting T-cell activation and release of vasoactive and proinflammatory cytokines implicated in the capillary leak and possibly also in myocardial impairment. The interaction between the NS1 and the glycocalyx layer of the vascular endothelium is thought to increase capillary permeability. The resulting plasma leakage may contribute to the cardiac dysfunction in the form of reduced preload, altered coronary microcirculation, and myocardial interstitial oedema. Altered intracellular calcium homeostasis has also been demonstrated in dengue infected myotubes. Abbreviations: DENV, dengue virus; NS1, nonstructural protein 1. (Yacoub et al., 2014)

Reference	Study population	*n*	Age	Country	Methods of cardiac assessment	Main findings
Yacoub *et al.* (2012)	Hospitalized adults and children: 22 dengue, 42 dengue with warning signs, 15 severe dengue	79	Median 20 years (range 8–46 years)	Vietnam	Echocardiography including tissue Doppler imaging, biomarker assessment (17 patients), ECG (51 patients)	Systolic impairment in 45% of patients, diastolic impairment in 42%. Septal and right ventricular walls predominantly affected, worse in severe cases. ECG abnormalities in 35% of 51 patients assessed. One patient had borderline troponin elevation, biomarker levels in the other 16 patients were normal
Wali *et al.* (1998)	Hospitalized older children and adults: nine DHF, eight DSS	17	Mean 29.7 years (range 14–58 years)	India	Echocardiography, radionucleotide ventriculography, Tc-pyrophosphate imaging (four patients), ECG (17 patients)	Mean LVEF was 41.7% using radionucleotide ventriculography, and 47.1% using echocardiography. Global hypokinesia detected in 12 patients (70.59%). Mean LVEF in patients with DSS was 39.63%. No myocardial necrosis detected in four patients using 99mTc-pyrophosphate imaging. ECG showed ST and T wave changes in 29.4% of 17 patients.
Khongphatt hanayothin *et al.* (2003)	Hospitalized children: four DHF grade I, 10 DHF grade II, 10 DSS	24	Mean 10.8 years (± 2.8 years)	Thailand	Echocardiography (VCFc/ESS)	Lower LVEF, VCFc/ESS, CI, EDV and higher SVR during critical phase versus recovery.
Miranda *et al.* (2013)	Hospitalized children and adults: 54 DF, 26 DHF grades I and II, one DSS	81	Mean 32 years (range 4 months to 81 years)	Brazil	Echocardiography (10 patients), biomarker assessment, CMR (four patients)	Raised biomarker levels in 15% of patients. 10 patients underwent echocardiography, four of whom had abnormalities, including functional and regional wall abnormalities. CMR showing myocardial enhancement in four patients.
Kabra *et al.* (1998)	Hospitalized children	54	<12 years	India	Echocardiography	LVEF was <50% in 16.7% of patients, and <35% in 3.7% of patients. No difference between severity grades.
Khongphatt hanayothin *et al.* (2007)	Hospitalized children: 30 DF, 36 DHF, 25 DSS	91	Mean 10.5 years	Thailand	Echocardiography, biomarker assessment (11 patients)	Reduced LVEF (<50%) was found in 6.7%, 13.8%, and 36% of patients with DF, DHF, and DSS during the critical phase, respectively. Biomarker levels were normal in all 11 patients tested.
La-Orkhun*et al.* (2011)	Hospitalized children	35	Mean 11.7 years (— 2.3 years)	Thailand	ECG 24 h Holter monitoring	During recovery phase, 29% of patients had ECG abnormalities including, sinus arrhythmias, first-degree and Mobitz type I second-degree AV block, and atrial and ventricular ectopic beats. No difference in severity between the groups.
Kularatne *et al.* (2007)	Hospitalized older children and adults	120	Median 34 years (range 13–76 years)	Srilanka	ECG, biomarker assessment (17 patients)	ECG abnormalities, including sinus bradycardia, T wave and ST-segment changes and right bundle branch block, in 62.5% of patients. Increased troponin levels in 29.4% of 17 patients tested.
Salgado *et al.* (2010)	Hospitalized children: 23 DF, 79 DHF	102	Mean 6 years (range 13 months to 10 years)	Colombia	Clinical assessment, echocardiography (seven patients), ECG (11 patients)	Myocarditis diagnosed clinically in 13.9% of 79 patients with DHF. ECG showed sinus bradycardia in 81.8% of 11 patients, tachycardia in 18.2% of 11 patients, and T wave inversion in seven of 11 patients. Echocardiography showed pericardial effusions in 71.4% of seven patients and diastolic dysfunction (parameters not specified) in 28.3% of seven patients.

Table 1.4: Studies of myocardial dysfunction in acute dengue (Yacoub et al., 2014).

2. Materials and methods

2.1 Buffers and solutions used in my thesis work:

Transformation Buffer 1 (Tfb1)

Reagent	Concentration
Potassium acetate (CH_3COOK)	30mM
Rubidium chloride ($RbCl_2$)	100mM
Calcium chloride ($CaCl_2$)	10mM
Manganese chloride ($MnCl_2$)	50mM
Glycerol	15%

Adjust pH to 5.8 with 0.2M acetic acid

Transformation Buffer 2 (Tfb2)

Reagent	Concentration
MOPS	10mM
Calcium chloride ($CaCl_2$)	75mM
Rubidium chloride ($RbCl_2$)	10mM
Glycerol	15%

Adjust pH to 6.5 with KOH

10X Protein running buffer

Reagent	Concentration
Tris base	30.2g/1 liter
Glycine	144g/1iter
SDS	10g/1 liter

Adjust pH to 8.3 with Conc. Hcl

6X Sample loading buffer for agarose gel electrophoresis

Reagent	Concentration
Bromophenol blue	0.25%
Xylene cyanol	0.25%
Glycerol	30%

4X Sample loading buffer for PAGE

Reagent	Concentration
Tris HCl (pH 6.8)	0.2M
SDS	0.8g/10ml
Glycerol	40%

β-Mercaptoethanol 14.7M	0.4ml/10ml
EDTA 0.5M	0.05M
Bromophenol blue	8mg/10ml

RIPA buffer

Reagent	Concentration
Tris HCl (pH 8)	50mM
NaCl	300mM
Glycerol	10%
Triton X-100	1%

10X PBS

Reagent	Concentration
KCl	2g/Liter
NaCl	80g/ Liter
KH_2PO_4	2g/ Liter
Na_2HPO_4	11.5g/ Liter

Adjust pH to 7.4 with 1N NaOH

STET Buffer

Reagent	Concentration
Sucrose	8%
Triton X-100	5%
EDTA	50mM
Tri base (pH 8.0)	50mM

CTAB buffer (5% w/vol)

Reagent	Concentration
CTAB	2g/100ml
Tris base (pH8.0)	0.1M
EDTA	0.2M
NaCl	1.4M
Polyvinyl pyrrolidone	1g/100ml

Adjust pH to 5.0 with HCl

Protein transfer buffer

Reagent	Concentration
Glycine	0.293mg/100ml
Tris base	0.582mg/100ml
10%SDS	0.375mL/100ml
Metanol	20%

Coomassie Blue

Reagent/ solvent	Concentration
Acetic acid	10%
Methanol	50%
Coomassie brilliant blue R-250	0.5g/ 200mL

Blocking solution

4.5% Nonfat milk powder in 1X PBS solution

Destaining solution

Reagent	Volume
Methanol	30%
Acetic acid	10%

Ponceau red staining solution

Reagent	Weight or Volume
Acetic acid	1%
Red Ponceau	0.5g/ 100mL

SOB medium

Reagent	Weight or Concentration
Tryptone	20g/ Liter
Yeast extract	5g/ Liter
NaCl	10mM
KCl	2.5mM

5X TBE Buffer

Reagent	Concentration
Tris base	1.1M
EDTA	25mM
Borate	900mM

Adjust pH to 8.3

2.2 Cell culture and transfections

H9c2 cells, (passage 17–30, American Type Culture Collection) were cultured in monolayers in DMEM (GIBCO) supplemented with 10% FBS (GIBCO), sodium bicarbonate 1.5 g/l, penicillin (50 IU), and streptomycin (50 µg/ml) under atmospheric conditions of 95% air and 5% CO2 at 37 °C in a humidified incubator. Stocks of cell lines were propagated in culture flasks for successive passage. Cells were used when they reached 80–90% confluence, usually within 24–48 h.

Constructs containing the β4b subunit cloned by Castellano et al(Castellano, Wei, Birnbaumer, & Perez-Reyes, 1993). or empty vector pSG5 plasmids were transiently transfected into H9c2 cells with Lipofectamine 2000 (Invitrogen) according to the manufacturer's instructions; the medium was replaced after 4–6 h and cultures were maintained for a total of 48 h. Poly(I:C) (Sigma), the synthetic analogue of double-stranded RNA with a molecular pattern associated with viral infection, was transfected at 50 or 100 µg/mL with Lipofectamine 2000 for 24 h according to the manufacturer's protocol. Control experiments involved the use of mock transfections with a 0.9% NaCl solution.

2.3 Preparation of competent cells

A single colony of *E. coli (DH5α)* was inoculated into 5 ml of SOB medium supplemented with 10mM MgSO4 and agitated overnight at 37 ^{0}C. 500 µl of initial culture was added to 50 ml of SOB containing 10mM MgSO4. The culture was grown at 37 ^{0}C with shaking at 200-250 rpm until it reached an optical density of 0.5 at 550 nm, after that culture was transferred on to ice for 10 min. This was followed by centrifugation at 4 ^{0}C with 2500 rpm for 12 min. After removing supernatant, cells were re-suspended in 16 ml of TFB1 followed by incubated on ice for 15 min and centrifuged again at 2500 rpm for 12 min at 4 ^{0}C. Cells were re-suspended in 4 ml of TFB2. After bacteria had been incubated on ice for 15 min, aliquots of 200 µl were made and stored at -70 ^{0}C.

2.4 A one tube plasmid DNA mini preparation

1 ml of final bacterial culture contacting plasmid was centrifuged at 14000 rpm for 1 min at room temperature. The bacterial pellet was mixed with 200 µl STET buffer, 10 µl lysozyme and 5 µl of RNAse followed by vortexed and incubated at 37 ^{0}C for 10 min. Samples were boiled and centrifuged for 1 min at room temperature at 14000 rpm. After removing pellet, 10 µl of CTAB (5 % w/V) detergent was added and mixed well followed by centrifuged at room temperature for 5 min at 14000 rpm. After removing supernatant 300 µl of 1.2 M of sodium chloride was added to the pellet and mixed well. 750 µl of ethanol was added for reprecipitation of DNA and centrifuged at room temperature for 10 min at 14000 rpm. After removing supernatant, final pellet was rinsed in 70% of 300 µl ethanol and centrifuged again for 5 mins. Dried pellet plasmid DNA was suspended with 50 µl of deionized water.

2.5 Agarose gel electrophoresis

Plasmids or DNA fragments were observed and separated in 0.8% agarose gels. Agarose was dissolved in 1xTBE buffer by heating in a micro oven for 2 to 3 minutes, and 1 µl ethidium bromide was added to visualize DNA. Gel solution was loaded into gel chamber allowed for solidification. DNA fragments or plasmids were mixed with 6x DNA loading buffer and loaded into the agarose gel. Plasmids or DNA fragments were separated at 80V in 1xTBE buffer for 40 min. Separated fragments were observed under UV illuminating box.

2.6 Bacterial transformation and plasmid isolation

Plasmids were added to 200 µl of competent *E. coli* thawed on ice. After 20 min incubation on ice, 90 seconds heat shock was applied at 42 ^{0}C, and then cells were placed on ice for 1-2 min. Transformation mixture was added to test tube containing 800 SOB medium supplemented with 16 µl of 20% glucose and 8 µl of 1M MgSO4 and cultured for 90 min at 37 ^{0}C and 180 rpm. After that bacteria were spread on to LB agar containing 100 µg/ml ampicillin. Plates were incubated overnight at 37 ^{0}C followed by stored at 4 ^{0}C.

A single colony of plasmid-containing bacteria was inoculated into 5 ml of TB dry containing 5 µl of ampicillin and was grown at 37 ^{0}C for 8 hours. Followed by 500 µl of start-up culture was diluted with 250 ml of TB dry containing 250 µl ampicillin and further grown overnight at 37 ^{0}C with vigorous agitation. Before plasmid preparation at large scale, a one tube plasmid DNA mini preparation was performed to measure that yield and quality of plasmid were appropriate. For larger scale plasmid preparation, QIAGEN plasmid maxi kit was applied.

2.7 Virus stock and viral infections

Propagation of four DENV serotypes: serotype 1 YUC18494 strain (clinical isolated from a patient with DENV, was kindly donated by Dr Isabel Salazar IPN-Mexico); DENV serotype 2 New Guinea strain; DENV serotype 3 H87 strain and DENV serotype 4 H241 strain, was carried out in CD1 suckling mice brains and titers were determined by plaque assays in BHK-21 cells as previously described (Mosso et al., 2008). CD1 suckling mice brains from mock-infected mice were used as a control.

For all experiments, cells were washed three times in Hank's solution and infected by exposure to DENV (serotype1, 2, 3 and 4) at an MOI of 5 or 10 in serum-free medium for 2 h at 37 ºC. Cells were washed with acid glycine (pH 3) to inactivate non-internalized virus, washed three times with PBS, and then serum-supplemented DMEM was added. The infection was permitted to proceed for 24 h or 48 h at 37 °C.

2.8 Confocal Immunofluorescence

H9c2 were grown on coverslips in 12-well plates for confocal microscopy. Cells were fixed with 1% formaldehyde 48 h postinfection, incubated for 20 min with permeabilizing solution (e.g., PBS, 0.1% saponins, and 1% FBS), and incubated for 2 h at RT with anti-NS3 primary antibody (1:10, GENTEX), followed by goat anti-rabbit-Alexa 555 (Life Technologies) secondary antibody (Life Technologies) for 1 h. To detect β4, monoclonal anti-CACNB4 (1:100, Abcam) primary antibody was applied followed by donkey anti-mouse-Alexa 488 (Life Technologies) secondary antibody for 1h. Slides were mounted with Vectashield® and labelled cells were observed through a Zeiss LSM700

imager.Z2 confocal laser microscope at RT. Images were acquired with a 40x objective (EC-PlanarNeofluar 40x/1.30 oil dichroic M27) and high-resolution camera Axiocam Hrm. Acquisition and analysis of images were performed with ZEN software, v. 2010.

2.9 Digital gene expression sequencing

Total RNA from H9c2 cells transfected with the β4 subunit or empty vector were isolated with an RNeasy Mini kit (Qiagen, Hilden, Germany). Gene expression profiling was conducted with Illumina next-generation sequencing technology (LCSciences, Houston, TX) on the Illumina HiSeq 2000 platform (1×50 bp SE, rapid mode). Gene expression data analysis was performed by LC Sciences and included log2 transformation.

2.10 Quantitative reverse transcriptase polymerase chain reaction (qRT-PCR)

Conventional RT-PCR from isolated RNA performed with DV2C-L 5´-CAA TAT GCT GAAACG CGA GA-3´and DV2C-R: 5´-TGC TGT TGG TGG GAT TGT TA-3´primers amplified a 151-pb fragment of the DENV capsid gene. The product was cloned in a pJet1.2 VectorSystem (Thermo). The recombinant plasmid was purified and quantified using spectrophotometry at 260 nm to prepare a dilution containing 1010 copies of plasmid/mL according to the formula:

No. copies = (6 × 1023 copies/mol × concentration (g/μl) / plasmid molecular weight) + insert (g/μl)

Serial dilutions of the plasmid (109 –102 copies/ml) were prepared. Reverse transcription was performed with 1 μg of total RNA from each experimental condition and random primers (Promega) at a concentration of 0.025 μg/μl and the reverse transcriptase enzyme ImpromII (Promega) at 25 °C for 5 min, 42 °C for 60 min, and 70 °C for 15 min. For real-time PCR amplification, SYBR Fast universal (Kapa) was used in an Eco Illumina System apparatus. The reaction mix contained 1 μl of cDNA and 5 μl of Master Mix 2×. The amplification protocol included 2 min at 50 °C, 2 min at 95 °C, and 40 cycles at 95 °C for 5

s, and 30 cycles at 55 °C. Finally, a dissociation curve was generated by heating the products from 55 °C to 95 °C to confirm primer dimer absence. A standard curve was generated.

To measure mRNA levels of antiviral factors and β4, RNA was isolated with the RNeasy Mini kit (Qiagen). Reverse transcription was performed with 500 ng of DNAse-treated RNA in 20-µl reactions. Synthesis of cDNA was carried out with Superscript III reverse transcriptase (Invitrogen) and random hexamers (250 ng) following the manufacturer's instructions.

The relative expression levels of mRNAs of β4, Irf7, Ifitm3, Ddx58, Stat2, Ifnb1, Mx1, and Ifih1 were quantified by TaqMan assays (Applied Biosystems, Foster City, CA). 18S ribosomal RNA (rRNA) was used as an internal control. Quantification was performed by the $2^{-\Delta\Delta Ct}$ method. This procedure is valid if the amplification efficiencies of the target and reference genes are approximately equal, as it was the case in our experiments.

2.11 Subcellular fractionation and quantification of proteins

H9c2 cells grown in p100 plates were trypsinized in 0.25% trypsin solution, and cells were collected by centrifuging at 850 rpm for 8 min. Nuclei and cytoplasm were separated by a nuclear complex co-ip kit (Active Motif) according to manufacturer's instructions. For whole-cell extracts, cells lysed with RIPA lysis buffer (300 mM NaCl, 50 mM Tris-HCl at pH 8.0, 1% Triton x-100, and 10% glycerol). Isolated protein content was quantified by Bradford's method.

2.12 SDS- polyacrylamide-gel-electrophoresis and western blot analysis

Equal amounts of proteins were separated by sodium dodecyl sulphate polyacrylamide gel electrophoresis and transferred to a nitrocellulose membrane (Bio-Rad). Membranes were blocked with 4.5% non-fat milk in PBS. Membranes were incubated overnight with primary antibody at 4 °C. After that, they were washed in PBS containing 0.1% Tween-20 and incubated in horseradish peroxidase-conjugated secondary antibody for 1 h at RT. Chemiluminescence was detected with Immobilon Western reagent (Millipore Co., Billerica, MA). The source of antibodies was: monoclonal anti-CACNB4 (1:500, Abcam; recognizes region close to the carboxy terminus between amino acids 458 and 474);

monoclonal anti-actin (1:2000, Sigma-Aldrich); polyclonal anti-Irf7 (1:1000, Abcam); anti-Ifitm3 (1:2000, Proteintech); polyclonal anti-Ddx58 (dilution, 1:1000; Abcam); polyclonal anti-histone H4 (1:1000, Abcam); polyclonal anti-β-tubulin (1:1000, Abcam); polyclonal anti-NS3 (1:1000, GeneTex); horseradish peroxidase-conjugated antimouse or anti-rabbit (Invitrogen).

2.13 Cytosolic calcium measurements and fluorescence imaging

H9c2 cells grown on coverslips were loaded with the cell-permeant fluorescent Ca^{2+} -indicator Fura-2- AM (Molecular Probes, Invitrogen, USA) for 45 min at RT. Fura-2-AM was diluted in PBS with 1 mM Ca^{2+} to a final concentration of ~ 5 µM (from a DMSO stock solution containing 9 mM Fura-2-AM, and 25% w/v Pluronic F127 (Molecular Probes). Cells were washed in PBS and left for 20–30 min at RT before performing $[Ca^{2+}]_i$ measurements. Ratiometric images of Fura-2 fluorescence were monitored using an Eclipse TE300 microscope (Nikon) equipped with a Polychrome V (TILL Photonics, Germany), which changed excitation wavelengths rapidly between 340 nm and 380 nm. Fluorescence emissions were captured through a 510WB80 filter (Chroma Technology Corp.) using an iXon EM+DU885 digital camera (Andor Technology, Belfast, UK). Image acquisition and ratio analysis were carried out in Imaging Workbench 6.0 software (INDEC Biosystems, USA).

2.14 Statistical analysis

Results data are expressed as means ± SEMs or SD. Statistical analyses were performed in GraphPad Prism 4.0 (GraphPad Software) and Sigma Stat 2.0; t-tests and one-way analyses of variance (ANOVAs) were used as appropriate. A $p < .05$ was considered statistically significant.

3. Results

3.1 Subcellular Localization of β_4 subunit in H9c2 cells

3.1.1 β_4 subunit is distributed in cytoplasmic and nuclear fractions of H9c2 cells

Western blot analysis of H9c2 cells demonstrated that expression of β_4 subunit protein was distributed in both cytosolic and nuclear fractions of control cells. Figure 2.1 A shows that in non-transfected cells the β_4 antibody recognized two protein bands (arrows) in both fractions. The lower band has a molecular weight of ~55 kDa that is close to the expected molecular weight of the β_4 subunit (58 kD). In addition, another faint band of slightly higher molecular weight was also detected. As expected, in transfected cells the density of both bands was greatly increased (Figure 2. 1 A). The purity of cytosolic and nuclear fractions was verified by the use of anti-tubulin and anti-histone antibodies (Figure 2.1 B-C). The cytosolic protein tubulin was only detected in the cytosolic fraction. Likewise, the nuclear protein histone was only observed in the nuclear fractions.

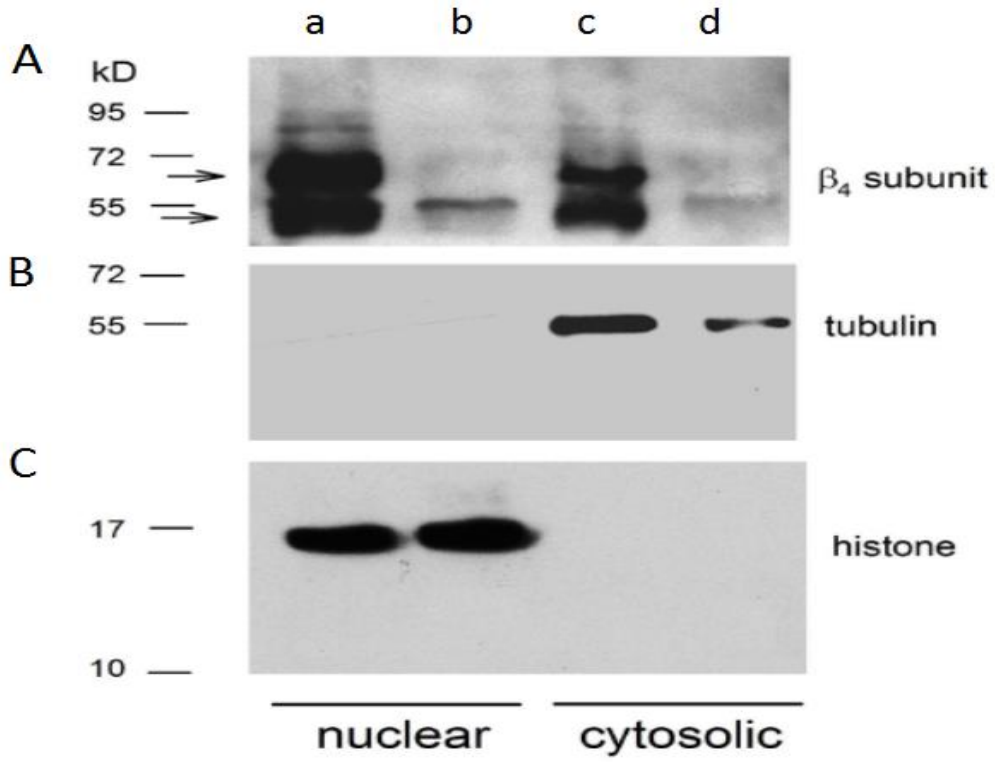

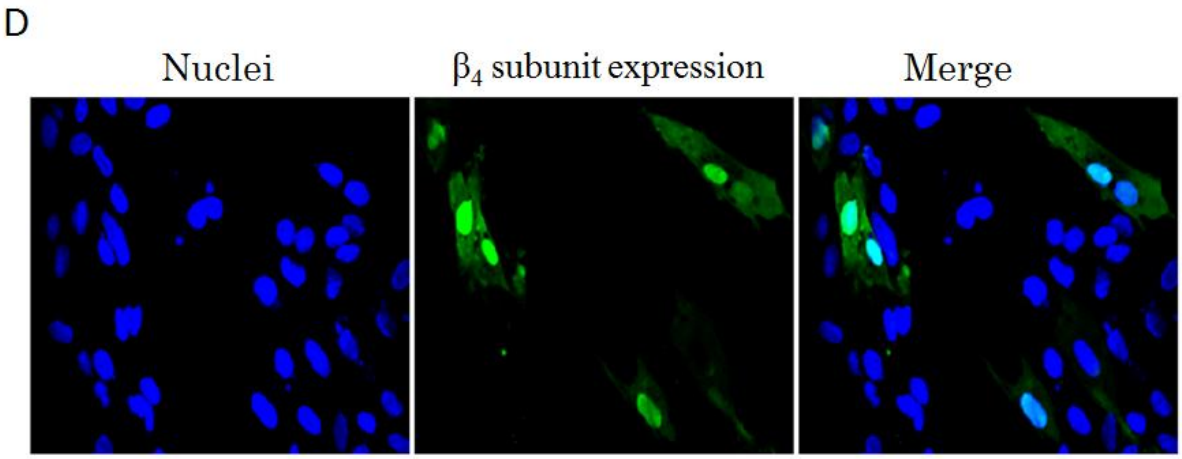

Figure 2.1: The β_4 subunit localizes in nucleus and cytoplasm of H9c2 cells. A: Representative western blots of the β_4 subunit. Lane a, nuclear fractions of cells transfected with β_4 subunit plasmid; lane b, nuclear fractions of cells transfected with empty vector plasmid; lane c, cytosolic fractions of cells transfected with β_4 subunit plasmid; lane d, cytosolic fractions of cells transfected with empty vector plasmid. B and C: western blots from the same samples probed with an anti-b-tubulin or anti-histone antibodies, respectively. (D) Localization of β_4 subunit in H9c2 cells transfected with a β_4 plasmid for 48 hr. The β_4 subunit was localized using anti-β_4 monoclonal antibody and with Alexa Fluor 488 conjugated antibody (green color). Nuclei were DAPI stained (blue color). Cells were examined using confocal microscopy.

3.2 β_4 subunit regulates the expression of antiviral genes

3.2.1 β_4 subunit regulates the expression of antiviral genes

Localization of the β_4 subunit in the nucleus of H9c2 cells raised the possibility that it regulates gene expression. Digital gene expression sequencing analysis confirmed this expectation. Table 2.1 shows results from control (vector transfected) and β_4 subunit over-expressed cells. As expected, the β_4 subunit (Cacnb4) was highly up-regulated by the transfection procedure. Other genes were also up-regulated, some related to transporters, ion channels, RNA binding, GTP binding, ATP binding protein, but the most noteworthy observation was the up-regulation of 50% of genes are related to the antiviral activity (Figure

2.2). Among these, there are three genes that encode proteins produced against viruses that are effective at different levels: Ddx58 (DEAD box polypeptide 58), Ifitm3 (interferon induced transmembrane 3) and Irf7 (interferon regulatory factor 7), a member of the interferon regulatory transcription factor family. Stat2 (signal transducer and activator of transcription 2, Mx1 (interferon induced GTP binding protein) and Ifih1 (cytoplasmic sensor of viral nuclear acids) were also significantly up-regulated.

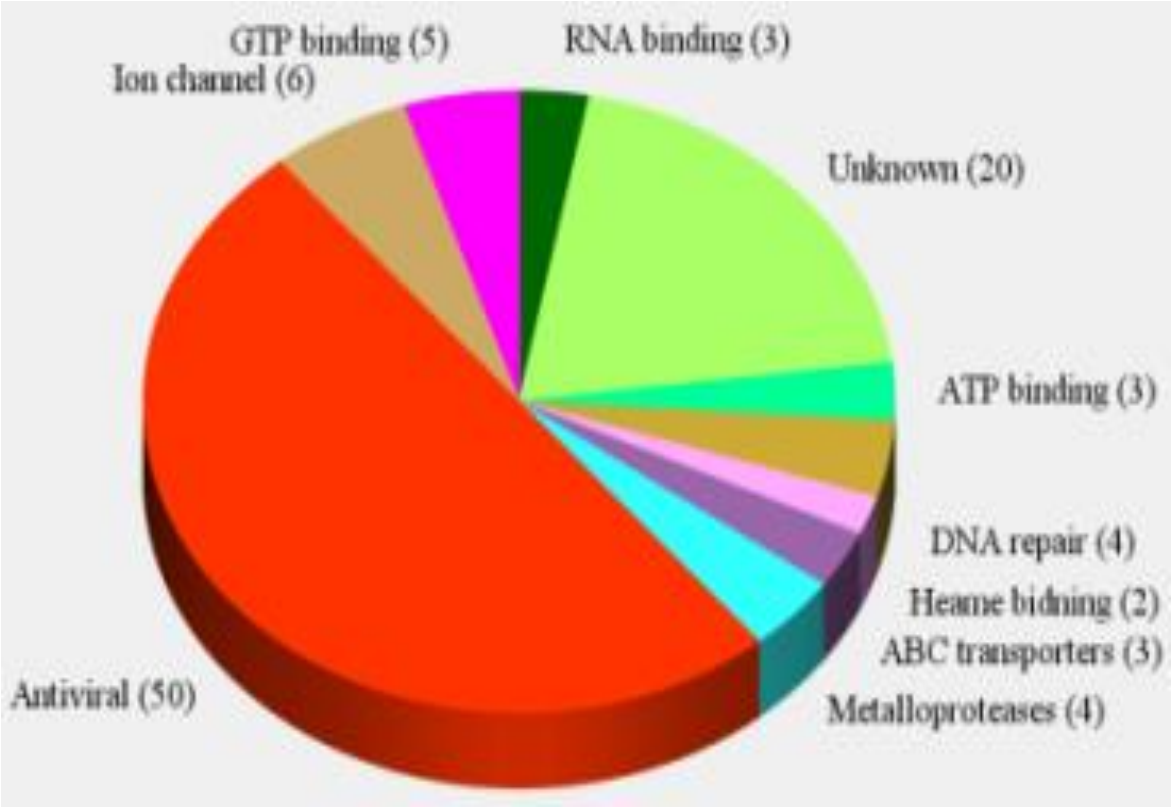

Figure 2.2: β_4 subunit over expression upregulates expression of a wide variety of genes related to different functions.

Table 2.1: Digital gene expression profiling analysis of genes regulated by β_4 subunit overexpression

gene	locus	Empty vector transfected	Beta4 Transfected	log2(fold_change)	p_value
Ifit2	chr1:238559728-238565793	10.49	132.81	3.66186	0.00E+000
Ifit3	chr1:238571299-238576441	22.30	427.70	4.26122	0.00E+000
Ifit1	chr1:238609169-238611236	26.19	289.51	3.46676	0.00E+000
Ifi47	chr10:34197629-34205260	0.69	17.30	4.65775	0.00E+000
Dhx58	chr10:89630144-89641311	3.60	42.39	3.55943	0.00E+000
Mx2	chr11:37548649-37572716	28.33	276.31	3.28602	0.00E+000
Oas1b	chr12:36858901-36869570	8.83	59.11	2.74286	0.00E+000
Oasl	chr12:42956465-42969826	13.85	113.14	3.03036	0.00E+000
Cxcl10	chr14:17198267-17280642	12.06	130.57	3.43707	0.00E+000
MGC108823	chr18:56250663-56259384	5.13	60.37	3.55775	0.00E+000
Ifi44	chr2:250039103-250056890	7.62	52.17	2.77577	0.00E+000
Cacnb4	chr3:33934477-34072070	4.37	6,265.98	10.4853	0.00E+000
Zbp1	chr3:164078443-164088795	4.29	67.52	3.9761	0.00E+000
Usp18	chr4:157692719-157694884	23.85	209.84	3.13701	0.00E+000
Ddx58	chr5:57597130-57645147	6.68	43.22	2.69316	0.00E+000
Isg15	chr5:173034478-173035766	17.96	285.08	3.98819	0.00E+000
Rsad2	chr6:44100774-44113910	1.88	19.83	3.39873	0.00E+000
Uba7	chr8:113244828-113253636	3.11	24.31	2.96612	0.00E+000
Oas1i	chr12:36760820-36772833	1.93	22.47	3.53822	2.22E-016
Tmprss2	chr11:37576800-37617258	0.51	9.52	4.20904	4.44E-016
RGD1309362	chr18:56154354-56179807	2.86	19.39	2.75928	8.88E-016
Ifitm3	chr1:201198658-201199768	148.13	819.51	2.46792	1.67E-014
Parp14	chr11:66736901-66768977	11.25	64.84	2.52728	2.07E-014
Rtp4	chr11:79433552-79445410	2.24	18.17	3.01953	2.31E-014
Bst2	chr16:18698547-18701768	3.47	50.12	3.85344	2.80E-014
Gbp2	chr2:240522999-240541078	19.64	102.82	2.38836	5.06E-014
Irf7	chr1:201456688-201459756	60.37	341.28	2.49906	8.50E-014
Tap1	chr20:4790362-4800730	13.75	68.30	2.3127	2.52E-013
Znfx1	chr3:158186219-158247372	6.55	36.80	2.4908	4.23E-013
Igtp	chr10:43829272-43837086	14.45	67.96	2.23323	1.32E-012
Stat2	chr7:1564384-1580652	25.72	127.50	2.30955	1.69E-012
Apol9a	chr7:115472724-115479486	48.21	229.10	2.24864	1.86E-012
Slfn3	chr10:71277764-71301183	2.63	12.95	2.29725	2.02E-012
Dtx3l	chr11:66649507-66659119	6.80	31.14	2.19476	2.86E-012

Oas1a	chr12:36806060-36816722	0.47	12.15	4.6916	5.01E-012
MGC105567	chr18:56363024-56383507	2.73	15.39	2.4938	6.92E-012
Irgm	chr10:34132511-34140450	3.18	17.10	2.42541	9.00E-012
Atf3	chr13:107191619-107223844	12.05	50.75	2.07429	9.57E-011
Mx1	chr11:37438472-37464077	0.38	25.85	6.10014	1.07E-010
Lgals3bp	chr10:108388184-108397520	65.91	289.29	2.13397	1.59E-010
Parp9	chr11:66615586-66648294	10.45	41.35	1.98495	2.37E-010
RT1-N3	chr20:2806582-2810443	12.59	50.98	2.01716	2.58E-010
Kcnt1	chr3:4050339-4088871	2.55	15.80	2.62984	6.31E-010
Trim34	chr1:162083188-162094690	5.68	22.84	2.00793	7.31E-010
Ifih1	chr3:44545560-44593969	1.76	12.14	2.79031	7.52E-010
Trim21	chr1:160174197-160187673	1.47	13.17	3.1654	1.21E-009
Trim25	chr10:77459829-77491594	3.99	14.55	1.86758	4.13E-009
RT1-A2	chr20:4998644-5060280	8.97	51.77	2.5285	2.78E-008
RGD1309808	chr7:115652325-115658693	8.41	33.39	1.98919	4.02E-008
Fam46a	chr8:90501686-90506133	2.84	10.44	1.87559	7.36E-008
Cd274	chr1:233053606-233065384	1.28	12.05	3.23086	1.29E-007
Slc8a1	chr6:4417928-4691719	0.00	5.03	1.80E+308	2.44E-007
Pnpt1	chr14:110130416-110161762	10.36	30.49	1.55767	5.18E-007
Hsh2d	chr16:18059419-18072483	0.30	3.11	3.38088	1.03E-006
Klrk1	chr4:166914785-166925222	0.22	4.23	4.23762	1.30E-006
Adamtsl3	chr1:138563869-138878648	2.09	6.25	1.57886	1.46E-006
Gbp5	chr2:240428471-240447783	0.63	3.20	2.34324	1.55E-006
Trex1	chr8:114071507-114072510	12.66	40.95	1.69327	1.94E-006
Lgals9	chr10:65129005-65152052	0.74	5.35	2.85614	2.04E-006
Ube2l6	chr3:68000238-68016331	16.96	48.17	1.50563	2.60E-006
LOC689064	chr1:161578126-161579492	63.98	19.29	-1.72942	2.69E-006
Cnksr1	chr5:152972550-152983208	1.04	4.82	2.20617	3.27E-006
Kcns3	chr6:34534528-34593882	3.31	0.03	-6.69008	6.28E-006
Isg20	chr1:134631523-134637868	33.38	90.82	1.44401	8.68E-006
Samhd1	chr3:147689046-147721246	7.79	20.68	1.40803	1.31E-005
Adamts19	chr18:54660287-54847297	2.16	0.49	-2.14022	1.43E-005

RT1-A1	chr20:4998644-5060280	3.23	27.30	3.07844	1.53E-005
Hbe2	chr1:161647650-161649279	37.29	9.68	-1.94564	2.28E-005
Tap2	chr20:4770445-4784488	5.59	15.34	1.45493	2.82E-005
Oasl2	chr12:42995885-43009399	1.68	25.45	3.91875	3.35E-005
C1s	chr4:160736132-160748137	4.03	10.71	1.41093	3.47E-005
Psmb9	chr20:4801186-4806608	0.14	8.44	5.94274	3.82E-005
Gdnf	chr2:57399191-57426615	6.07	15.71	1.37128	5.77E-005
Trafd1	chr12:36301823-36315741	22.78	53.64	1.23557	6.50E-005
Daxx	chr20:5121853-5127601	22.34	52.53	1.23335	6.69E-005
Itpr1	chr4:143705359-144030052	1.14	5.72	2.33242	6.73E-005
RT1-CE10	chr20:3468601-3471619	1.98	8.95	2.17496	8.26E-005
Rnf114	chr3:158650309-158662425	47.55	112.55	1.24293	8.27E-005
Casp12	chr8:2082932-2110511	15.57	37.15	1.25433	8.57E-005
Slfn2	chr10:71236407-71242745	19.15	43.66	1.18925	1.25E-004
Tnnt3	chr1:202745139-202762149	0.00	6.28	1.80E+308	1.30E-004
Ndrg2	chr15:27338551-27347191	0.00	1.21	1.80E+308	1.35E-004
Tmem106a	chr10:90602483-90611299	1.49	4.58	1.62063	1.53E-004
Abcc10	chr9:10219821-10244071	0.00	1.20	1.80E+308	1.71E-004
Palmd	chr2:213174872-213228299	29.24	65.44	1.16208	1.76E-004
Mitd1	chr9:36827856-36839148	10.83	25.97	1.26146	1.89E-004
Fbxw17	chr17:20268227-20286022	3.17	9.08	1.51675	2.05E-004
Nmi	chr3:32973351-32996031	13.00	32.42	1.31816	2.30E-004
Plekha7	chr1:174249021-174316226	19.74	46.29	1.22984	2.49E-004
Myh3	chr10:53776857-53800677	1.86	4.57	1.29689	2.54E-004
Pappa	chr5:81826648-82096446	2.33	5.54	1.25128	2.64E-004
Adamts15	chr8:30683280-30706659	0.32	1.17	1.85715	2.80E-004
Smndc1	chr1:259596307-259607378	0.00	9.59	1.80E+308	3.11E-004
Sgk1	chr1:23501257-23509096	7.28	18.92	1.37842	3.20E-004
Col6a2	chr20:12436782-12464512	2.09	0.57	-1.88676	3.25E-004
Ccrl2	chr8:115451785-115454088	0.25	1.53	2.59538	3.73E-004
Tmprss2	chr11:37576800-37617258	0.35	3.16	3.15423	3.95E-004
Cnp	chr10:89519418-89525978	18.10	38.77	1.09915	4.03E-004
Usp25	chr11:15799828-15907792	14.89	31.79	1.0937	4.31E-004

3.2.2 Validation of digital gene expression profiling analysis data of antiviral genes using qRT-PCR

In agreement with the gene expression profiling analysis results, analysis of mRNA abundance measured by qRT-PCR indicated that expression levels of all these antiviral factors (Irf7, Ifitm3, Ddx58, Stat 2, Ifnb1, Mx1 and Ifih1) were significantly increased by overexpression of the β_4 subunit relative to the levels observed in the control samples, as illustrated in Fig. 2.3

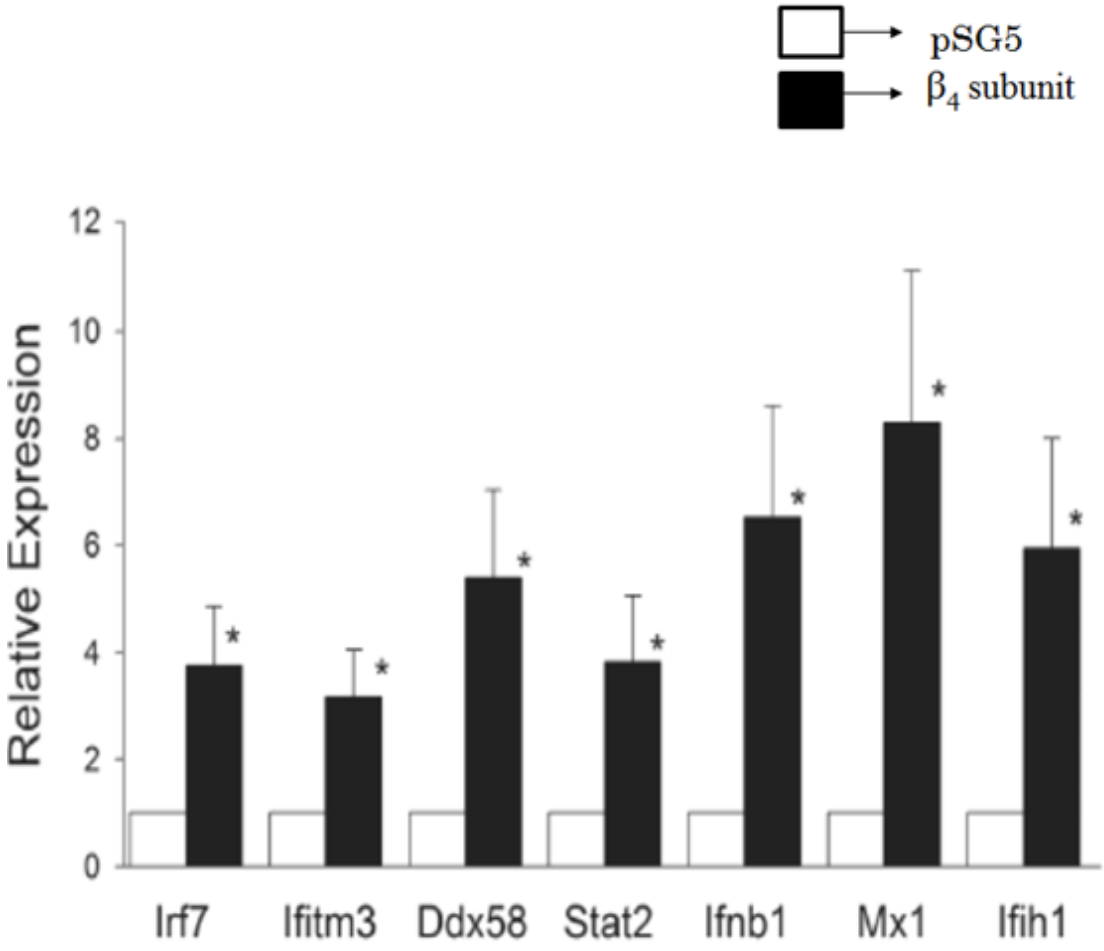

Figure 2.3: Validation of gene expression profiling data of β_4 subunit enhancing antiviral genes at mRNA levels. Quantitative analysis of mRNA expression of antiviral factors in H9c2 cell lysates from control (open bars) and β_4 subunit transfected cells (filled bars) (n = 9, *p < .05). All values are group means ± SEs.

3.2.3 β4 subunit overexpression enhances expression of antiviral factors at protein level

To determine whether antiviral factors are also up-regulated at the protein level, we performed western blot analysis to check the expression of Irf7, Ifitm3 and Ddx58 proteins and found that indeed their expression is significantly increased relative to controls by overexpressing the β4 subunit, as illustrated in Fig. 2.4 A-C. The protein expression levels of actin were not affected by β4 subunit and were used to normalize band densities. Fig. 2.4 D-F summarizes data from similar experiments. The expression of Ddx58 and Irf7 increased by 50% whereas that of Ifitm3 increased more than double.

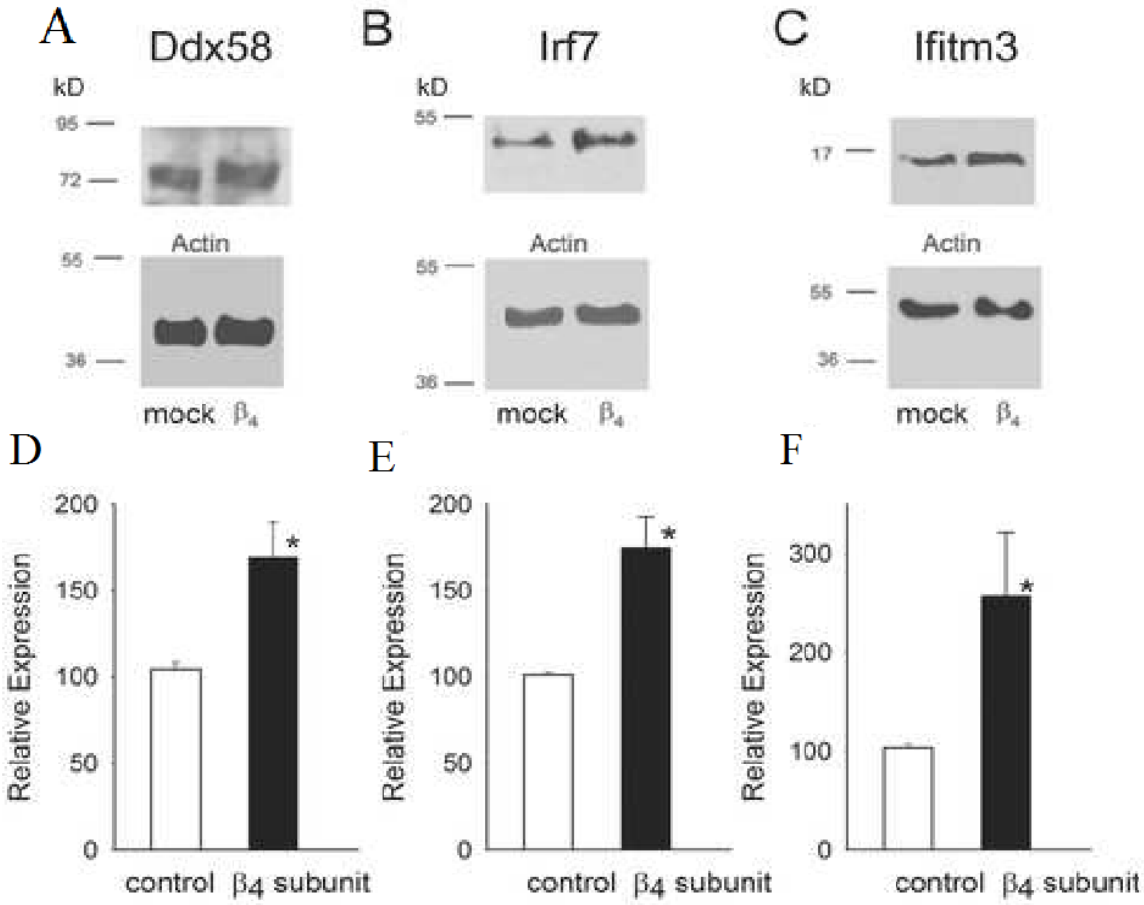

Figure 2.4: Over expression of the β4 subunit enhances expression of antiviral proteins. *A-C*: representative western blots of the indicated antiviral proteins and actin of the whole cell fraction of H9c2 cells under control conditions (left lanes) and from β4 subunit overexpressed cells (right lanes). D-F: Relative expression values of Ddx58, Irf7 and Ifitm3

under control conditions (empty bars) and from β_4 subunit transfected cells (filled bars). Values represent mean ± SD, n = 3-5, *$p < .05$.

3.3 Overexpression of the β_4 subunit reduces infection levels

3.3.1The four Dengue virus (DENV) serotypes can infect H9c2 cells

To check antiviral activity of β_4 subunit in H9c2 cells against Dengue virus infection, we initially address the susceptibility of H9c2 cells to DENV. The cells were infected with DENV serotype 1 YUC18110 strain (clinical isolate from a patient with DENV in Yucatan, Mexico), DENV serotype 2 New Guinea strain, DENV serotype 3 H87 strain and DENV serotype 4 H241 strain at an MOI of 1 for 24 h and the presence of the non-structural protein 3 (NS3) was monitored by western blot (Figure 2.5). The anti-NS3 antibody was able to recognize the NS3 protein from the four DENV serotypes infected cell extracts. However, the intensity of the bands was different. Bands detected in DENV1 and DENV2 infected cell extracts were more prominent than the ones detected in DENV3 and DENV4 infected cell extracts. Differences in the NS3 protein abundance, as well as differences in the affinity of the antibody to the NS3 proteins from the different DENV serotypes are probably responsible for the differences detected in the Western-blot assays.

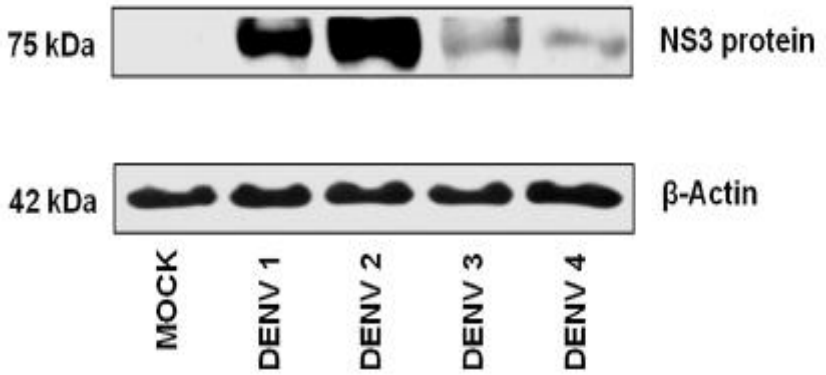

Figure 2.5: H9c2 cell line is susceptible to DENV infection. H9c2 cells were infected with the four DENV serotypes and viral infection was monitored by western blot using an anti-NS3 protein antibody.

3.3.2 The β_4 subunit decreases the expression of NS3 viral protein in DENV-2 infected H9c2 cells

We found with western blot analysis that the viral protein NS3 was down-regulated by the β_4 subunit. Figure 2.6A shows representative blots of NS3 from DENV-2 infected cells. The band corresponding to NS3 was significantly fainter by the over-expressed β_4 subunit (lane c) than those of control or empty vector transfected cells (lanes a-b). Results from similar experiments are summarized in Figure 2.6 B. The β_4 subunit reduced NS3 expression to a third the control value.

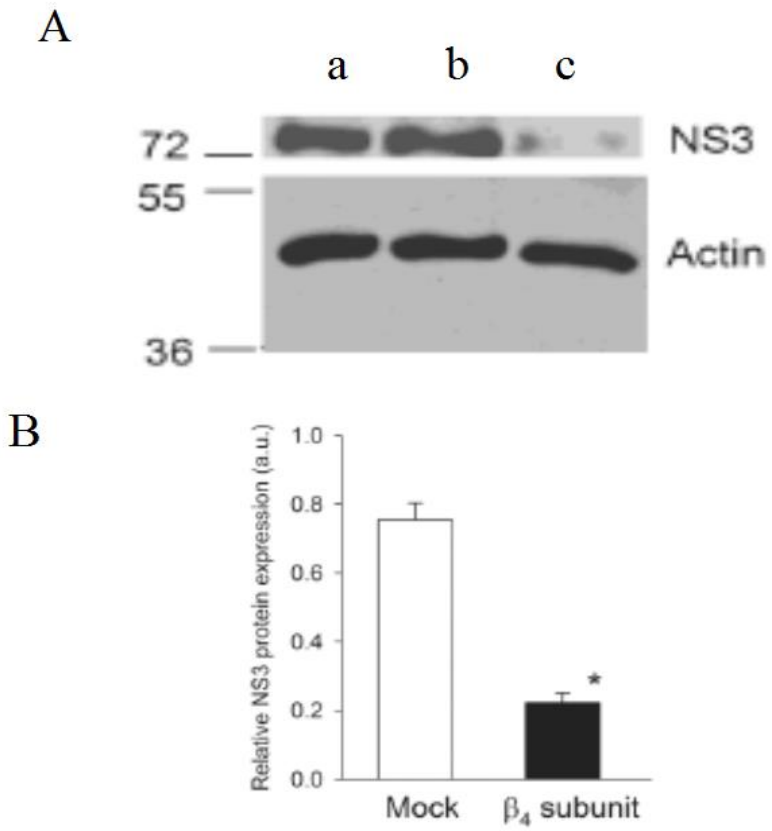

Figure 2.6: The β_4 subunit reduces the expression of the non-structural viral proteins NS3 in DENV-2 infected H9c2 cells. A: Representative western blots of NS3 viral protein from whole cell extracts of DENV-2 infected cells (MOI=5). Lane a: non-transfected cells. Lane b: cells transfected with empty vector plasmid. Lane c: cells transfected with β_4 subunit plasmid. B: Bars represent relative expression of NS3 viral protein from western blot data.

Open bars, empty vector results. Filled bars, results from β4 subunit transfected cells. Values represent the mean ± SD, n = 4, *$p < .05$.

3.4 Infection induces endogenous β4 subunit

3.4.1 Poly (I:C) transfection increases the expression of β4 subunit

We tested the hypothesis that the expression of β4 subunit in H9c2 cells increases when challenged with the double-stranded RNA, Poly (I:C) and found that indeed, a significant increase in β4 subunit expression was observed by Poly (I:C) transfection. Figure 2.7A illustrates representative β4 subunit immunoblots of the nuclear fraction from non-transfected H9c2 cells (control) and cells transfected with Poly (I:C). While poly (I:C) significantly increased the thickness of the β4 subunit band, no significant changes in the density of the actin bands were seen and these were used for normalization. Figure 2.7B summarizes results from similar experiments. Poly (I:C) more than doubled the expression of β4 channel subunit. As expected, the increase in protein levels was accompanied by a significant increase in the mRNA levels of the β4 subunit, as revealed by qRT-PCR experiments (Figure 2.7C). The messenger level increased more than 4 fold.

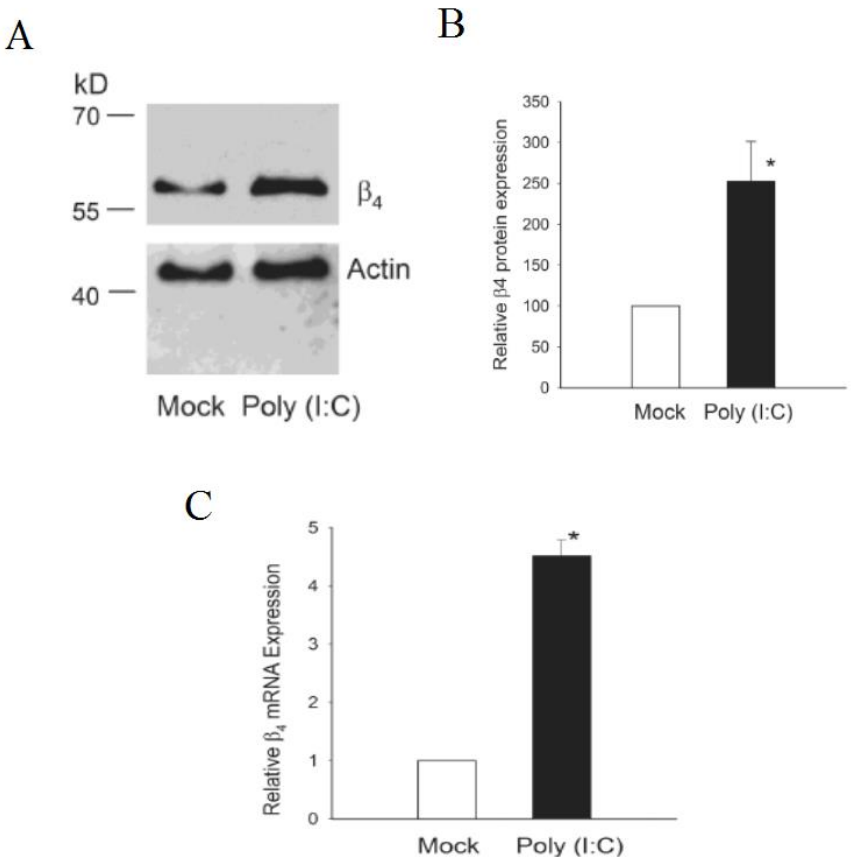

Figure 2.7: Poly (I: C) enhances the expression of β_4 subunit at protein and mRNA levels. A: representative western blots of the β_4 subunit and actin of the nuclear fraction of H9c2 cells transfected for 24 h with poly (I:C) or mock transfected. B: relative increase of β_4 subunit protein expression in poly (I:C) transfected cells (filled bar) and mock transfected cells (empty bar). C: mRNA expression of β_4 subunit with poly (I:C) transfection (filled bar) relative to control (empty bar). Values represent the mean ± SD, n = 3-5, $*p < .05$.

3.4.2 Poly (I:C) enhances translocation of β_4 subunit to the nucleus

Confocal microscopy revealed that Poly (I:C) preferentially increased the nuclear expression of β_4 subunit in H9c2 cells. Figure 2.8A illustrates the distribution of β_4 subunit under control conditions (upper panel, in green). When this image was merged with that of nuclei (upper panel, in blue), it became apparent that β_4 subunit can be found associated either with nuclei or the cytosol (Figure 2A, upper panel, right). A different picture emerged when Poly (I:C) transfected cells were analyzed. Poly (I:C) transfection greatly increased the expression of β_4 subunit as shown in Fig. 5 A (lower panel), but this Ca^{2+} channel subunit was preferentially associated to nuclei (lower panels). Figure 2.8 B and C summarizes these results. Figure 2.8B shows that Poly (I:C) increased the expression of β_4 subunit by ~3 fold, as revealed by the increase in mean fluorescence. Meanwhile, the localization ratio (nucleus/cytoplasm) increased ~ 7 fold by Poly (I:C) (see Figure 2.8C).

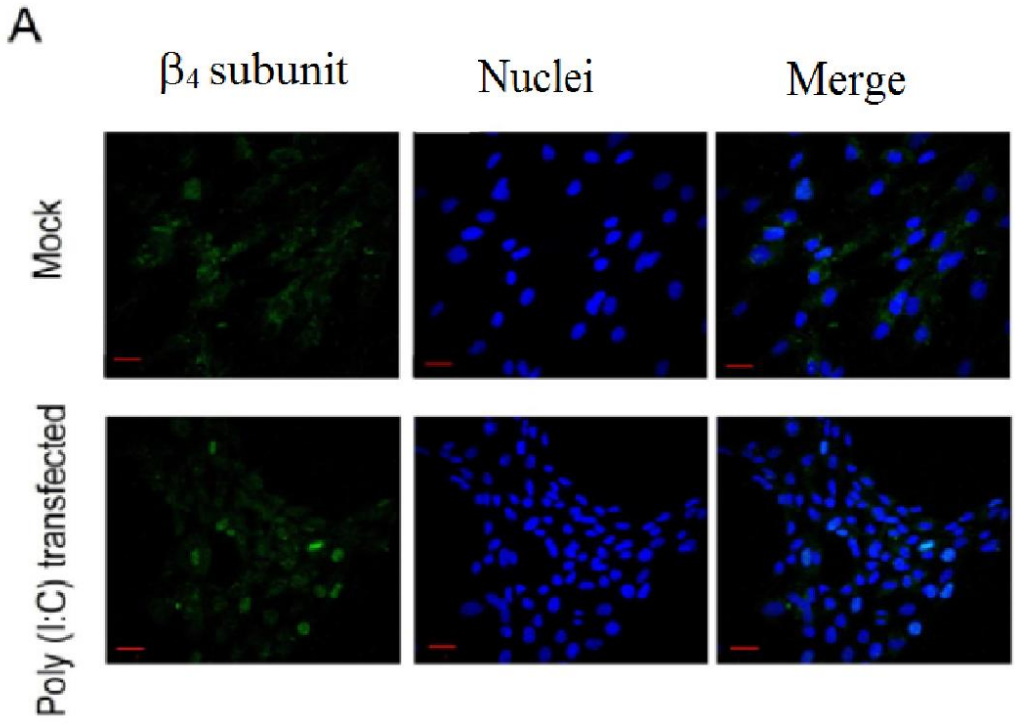

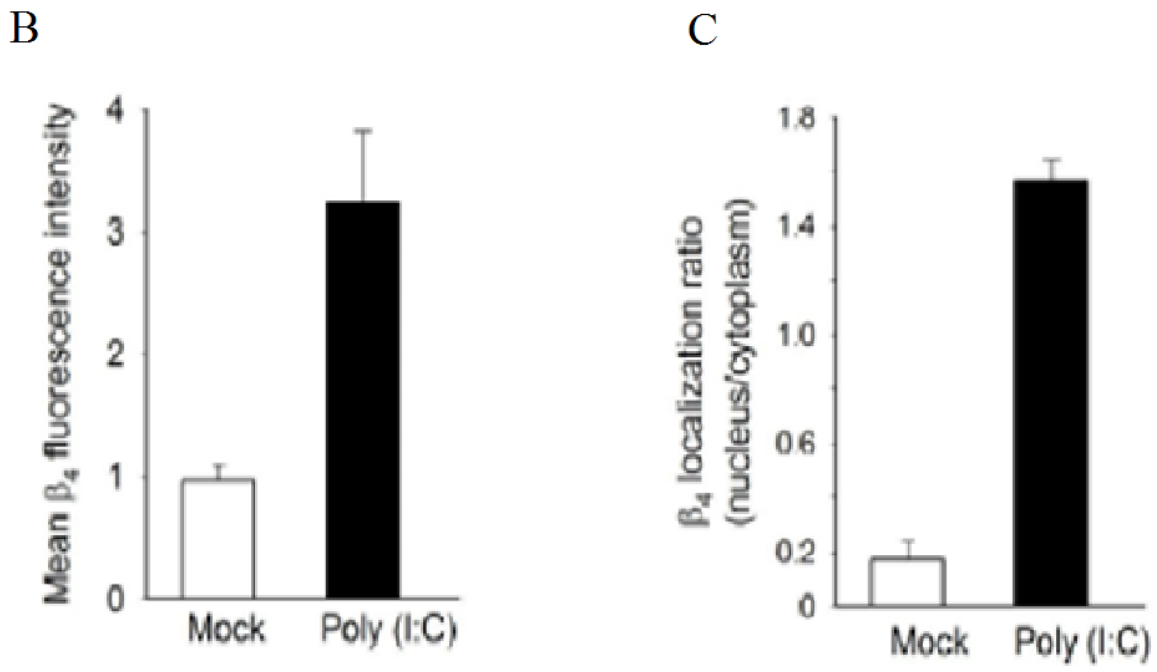

Figure 2.8: The β_4 subunit preferentially localizes in nuclei in response to poly (I:C) treatment. A: H9c2 cells transfected with poly (I:C) (100µg/ml) (lower panels) for 24 h or mock transfected (upper panels). The β_4 subunit was localized using anti-β_4 monoclonal antibody and with Alexa Fluor 488 conjugated antibody (green color). Nuclei were DAPI stained (blue color). Cells were examined using confocal microscopy. B, bars show relative expression of β_4 subunit in poly (I:C) transfected and mock transfected cells. C, bars show nucleus to cytoplasmic expression ratio of β_4 in poly (I:C) transfected and mock transfected cells. Values represent the mean ± SD, n = 3-5, $*p < .05$.

3.4.3 Dengue infection enhances the expression of β_4 subunit

Western blot analysis revealed that dengue infection significantly increased the expression of β_4 subunit while actin levels remained unaffected by the infection. Figure2.9A shows representative blots from the cytosolic fraction of DENV-2 H9c2 infected cells. Illustrated are immunoblots of β_4 subunit under control conditions (lane a) and of the β_4 subunit from MOI=5 (lane b) and MOI=10 (lane c) infected cells. In both cases, infection increased the expression of β_4 subunit almost 2 fold. DENV-2 infection also increased the expression of the β_4 subunit of nuclear fractions but only at MOI=10, as shown in Figure 2.9 C-D. Furthermore, DENV-2 infection also increased β_4 subunit mRNA levels significantly, with

the infected group having an expression level ~4 fold larger than that of the control group (Figure 2.9 E).

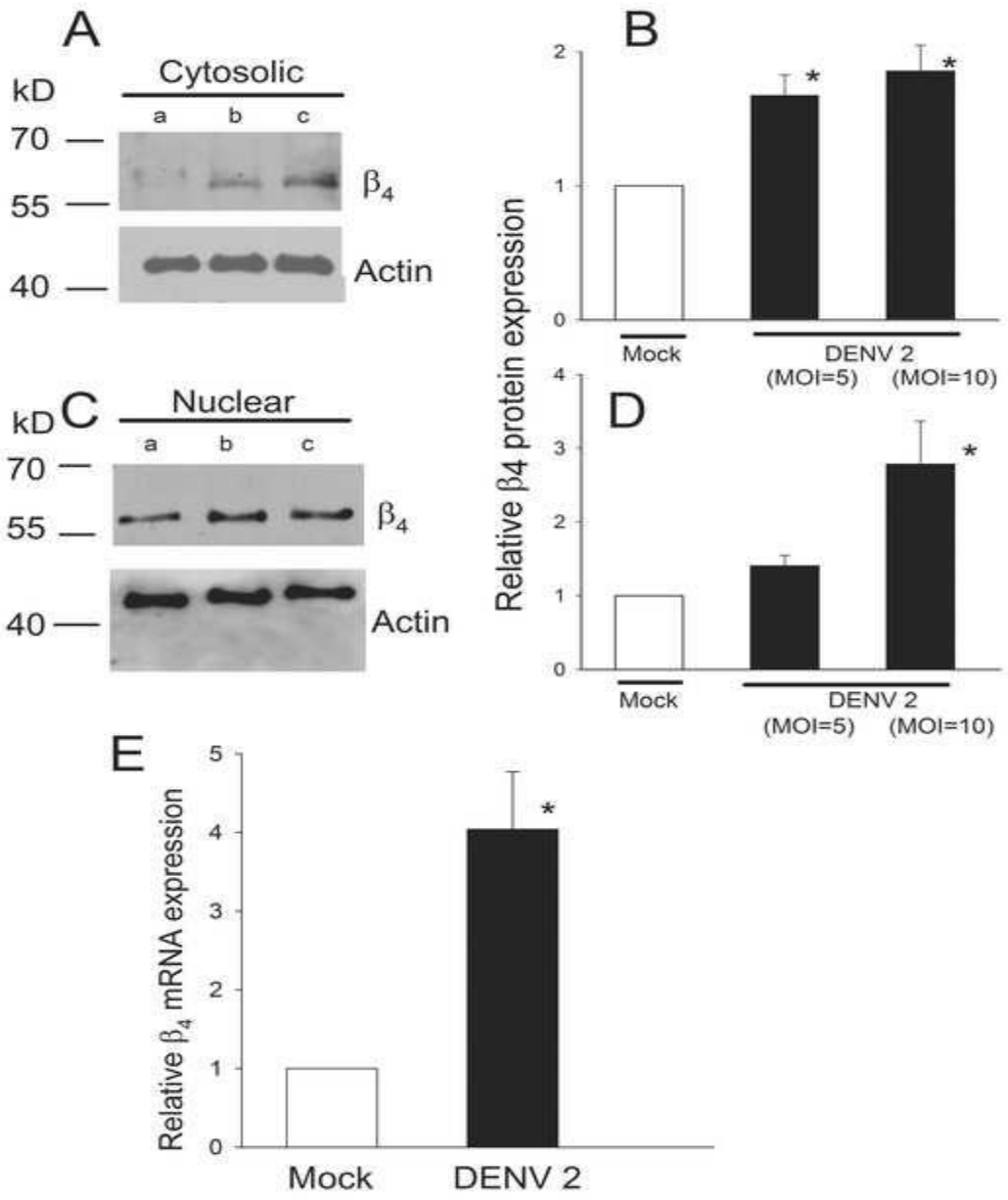

Figure 2.9: DENV 2 infection increases the expression of the β_4 subunit in H9c2 cells. Blots show β_4 (upper panel) and actin (lower panel) in cytosolic (A) and nuclear (C) fractions of H9c2cells. Cells were mock-infected (a) or infected with DENV2 at an MOI 5 (b) or an MOI of 10 (c). Relative expression of the β_4 in cytosolic (B) and nuclear (D) fractions of mock-infected (empty bar) or DENV-infected (filled bars) cells. (E) qRT-PCR analysis of relative expression of β_4 mRNA of mock infected (empty bar) and DENV2-infected cells (filled bar, MOI = 5). All data reported as mean values ± SD, *n* = 3-5 per group. *p < .05.

3.4.4 Dengue infection promotes the expression of β4 subunit in the vicinity of infection

To further examine the effects of dengue infection on the expression of the β4 subunit, confocal microscopy analysis was performed. A representative set of experiments is illustrated in Figure 2.10. The panels in A show images of DENV-2 infection (in red) at two different MOIs. In B, the presence of β4 subunit is illustrated (in green), and nuclei are shown in C (in blue). When images were merged, it was clear that the brightest green images were seen in nuclei of cells that were close to infection sites (1 and 2 in Figure 2.10 D). In non-infected cells, the β4 subunit appears in both cytosol and nucleus with no major preferential distribution (panel B). In contrast, infection not only brought about an overall increase in the expression of the β4 subunit but also led to its translocation to the nucleus. To support this conclusion, cells (labeled 1-4 in Figure 2.10D) were analysed. Results are shown in Table 2.2. We found that the ratio between β4 subunit in the nucleus to that in cytosol was close to 2 in non-infected cells. Whereas, this ratio increased to 6 or 11 in cells that were close to infection but remained low in cells located far from infection sites.

	Cell	β4 total MFI (a.u.)	β4 colocalization (nuclei)	β4 MFI (nuclei)	β4 MFI (cytoplasm)	β4 ratio (nuclei/cytoplasm)
Mock	1	2.44	0.68	1.632	.768	2.125
	2	4.48	0.718	3.217	1.263	2.546
	3	4.35	0.667	2.901	1.448	2.003
	4	4.43	0.676	2.995	1.435	2.086
Denv 2 (MOI 5)	1	48.66	0.931	45.302	3.357	13.492
	2	42.61	0.850	36.645	5.965	6.142
	3	11.23	0.589	6.614	4.615	1.433
	4	6.08	0.520	3.162	2.918	1.083
Denv 2 (MOI 10)	1	44.31	0.921	40.809	3.500	11.658
	2	22.19	0.865	19.194	2.995	6.407
	3	5.26	0.571	3.003	2.256	1.331
	4	10.01	0.633	6.336	3.673	1.724

Table 2.2: Distribution of β4 subunit near infection sites.

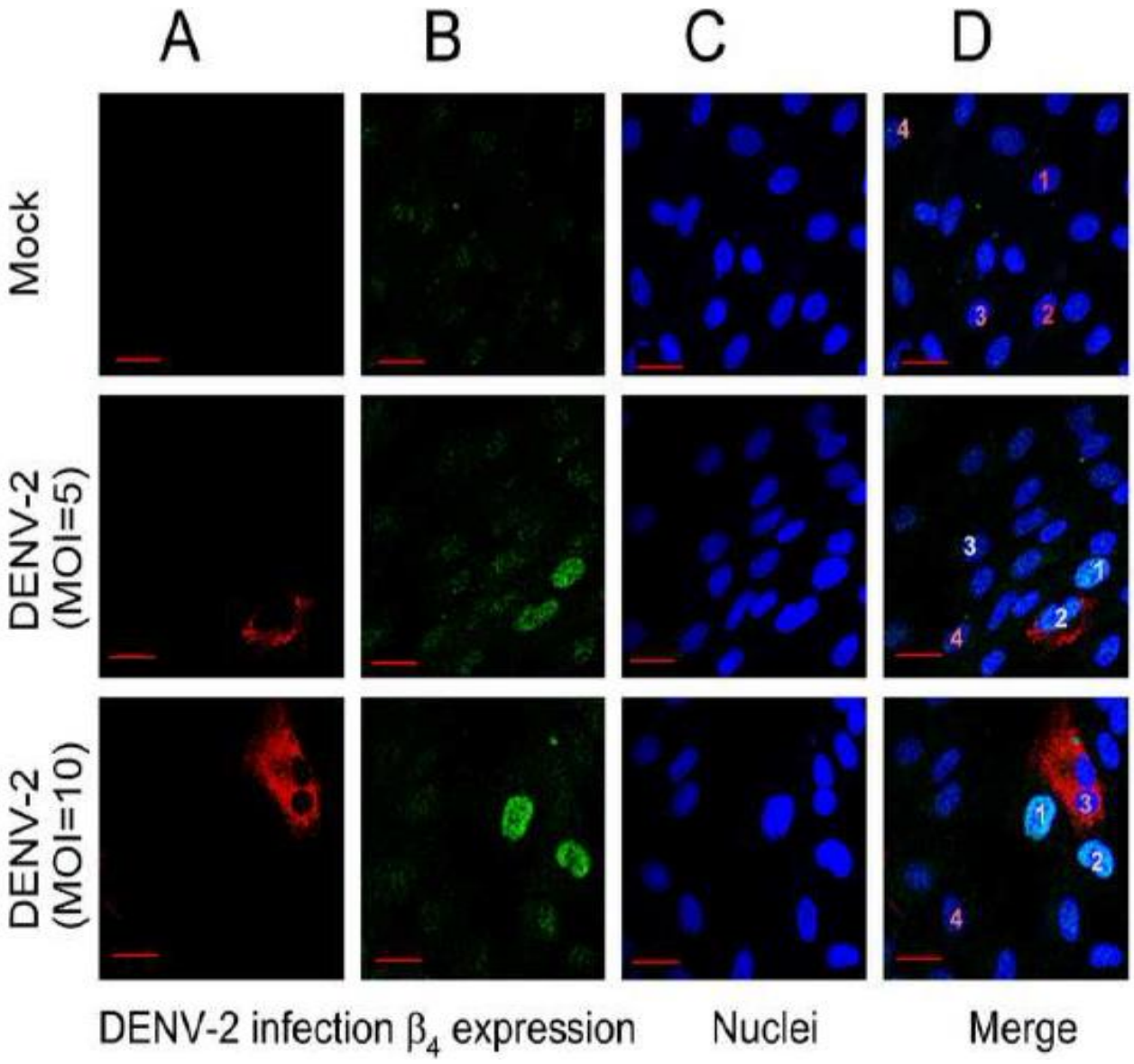

Figure 2.10: β_4 subunit expression in nuclei is enhanced in the vicinity of DENV 2 infected cells. H9c2 cells were mock infected (upper panels) or infected for 48 h at an MOI of 5 (middle panels) or 10 (lower panels) with DENV 2. The β_4 subunit was localized using anti-β_4 monoclonal antibody and with Alexa Fluor 488 conjugated antibody (green colour). Nuclei were DAPI stained (blue colour). NS3 viral protein expression was detected using a polyclonal anti-NS3 antibody (red colour). Cells were examined using confocal microscopy.

3.4.5 Soluble factors released during dengue infection enhance β4 subunit expression

Since β4 subunit was readily induced in cells which are in proximity of infected cells, we studied the effect of soluble factors which are released from infected cells. To study the involvement of soluble factors on the increased expression of β4 subunit during infection, H9c2 cells were treated with either concentrated supernatants of DENV-2 infected H9c2 cells or with supenatants from mock-infected cells. β4 levels were analyzed using confocal microscopy analysis. Figure 2.11 illustrates cells treated with DENV-2 infected supernatants (lower panel, in green). The treatment greatly increased β4 subunit expression in comparison with cells treated with the supernatant from mock-infected cells (upper panel, in green).

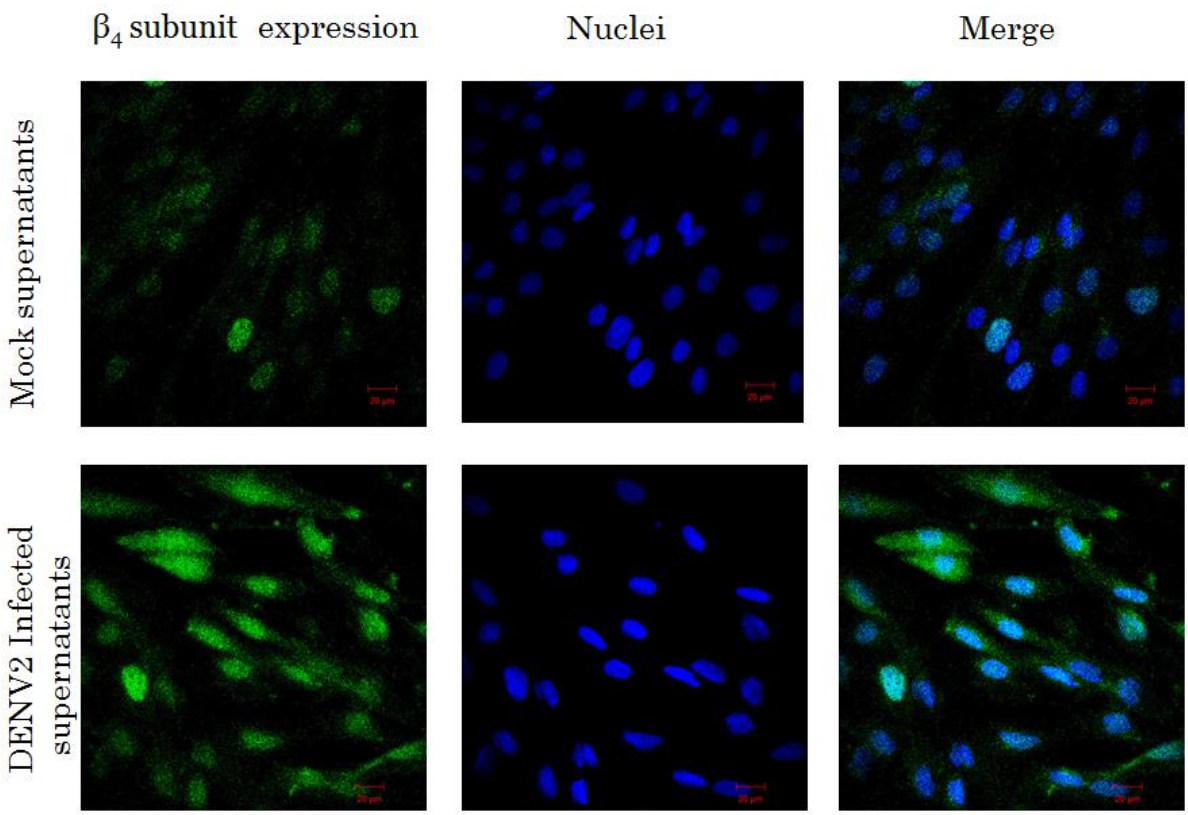

Figure 2.11: Soluble factors released during DENV-2 infection enhances the expression of β4 subunit. H9c2 cells were infected with DENV2 (MOI = 10) or mock infected for 10h. After infection, the supernatants were collected and added to a fresh batch of H9c2 cells and incubated for 48 h to examine β4 subunit expression. Confocal microscopy images of H9c2 cells treated with supernatants from infected cells (lower panels) or from mock-infected cells (upper panels). The β4 subunit was detected using anti-β4 monoclonal antibody and Alexa Fluor 488 conjugated antibody (green colour). Nuclei were DAPI stained (blue colour).

3.4.6 Interferon β (IFNβ) treatment enhances expression of β_4 subunit

Although the involvement of a soluble factor promoting the increase in the expression of β_4 subunit in H9c2 cells is most likely, as suggested by the effects of supernatants extracted from dengue infected H9c2 cells, its nature is still unresolved. Interferon β (IFNβ) an important cytokine is certainly a possible candidate. Therefore, we studied the effect of IFNβ on the expression of β_4 subunit using confocal fluorescence and western blot methods. Figure 2.12A and 2.12C illustrate representative β_4 subunit immunoblots of the cytosolic and nuclear fractions from cells treated with IFNβ (for 48 h) and untreated cells. While IFNβ treatment significantly increased the thickness of the β_4 subunit band both in cytosolic fractions and nuclear fractions, no significant changes in the density of the actin bands were seen and these were used for normalization. Figure 2.12E confocal microscopy images represents enhanced distribution of β_4 subunit both in both cytosolic and nuclear fractions under IFNβ treated condition (lower panel, in green) compared to that of untreated condition (upper panel, in green).

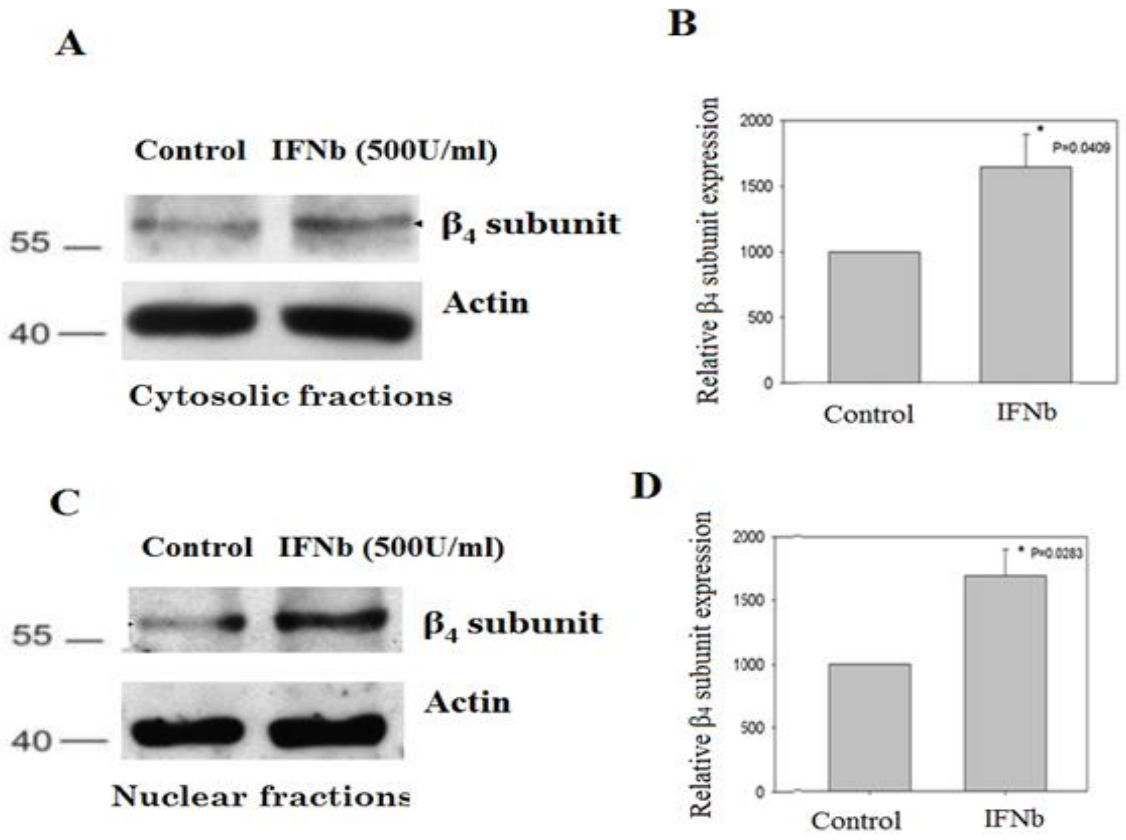

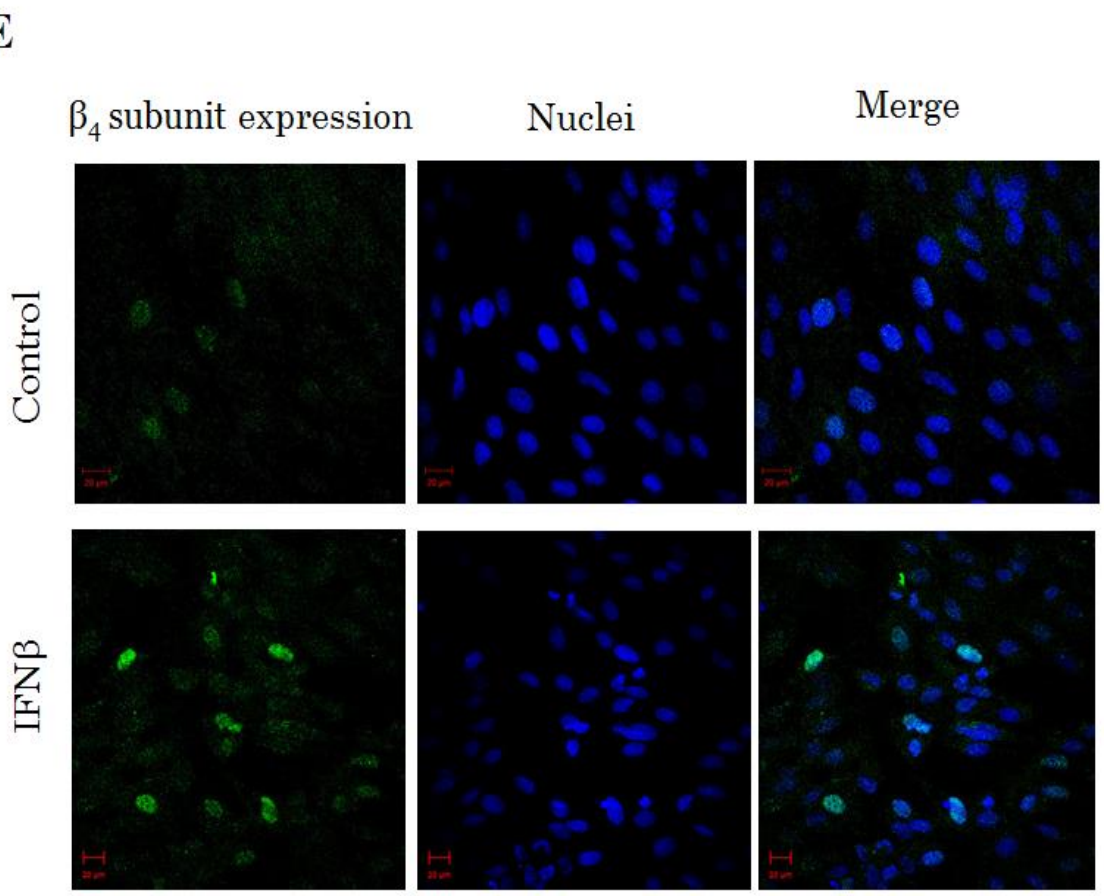

Figure 2.12: Intereferon treatment enhances expression of β_4 subunit in H9c2 cells. Blots show β_4 subunit (upper panel) and actin (lower panel) in cytosolic (A) and nuclear (C) fractions of H9c2cells. Cells were untreated or treated with IFNβ at concentration of 500 U/ml for 48 h. Relative expression of the β_4 subunit in cytosolic (B) and nuclear (D) fractions of untreated or IFNβ treated cells showed in bars. (E) Confocal microscopy images show H9c2 cells untreated (upper panels) or treated with IFNβ (lower panels) at 500U/ml concentration for 48 h. The β_4 subunit was localized using anti-β_4 monoclonal antibody and with Alexa Fluor 488 conjugated antibody (green colour). Nuclei were DAPI stained (blue colour). All data reported as mean values ± SD, *n* = 3-5 per group. *p < .05.

3.4.7 JAK1 inhibitor treatment downregulates β4 subunit expression

In order to further study the role of IFN and its downstream signaling pathway on expression of β4 subunit, we treated H9c2 cells with JAK1 inhibitor (GLPG0634) and studied expression of β4 subunit. Figure 2.13A illustrates representative β4 subunit immunoblots of the whole cell fractions from cells treated with JAK1 inhibitor and untreated cells. JAK1 inhibitor treatment repressed the expression levels of β4 subunit protein in a concentration dependent manner. Results from similar experiments are summarized in Figure 2.13B. Furthermore, qRT-PCR experiments revealed that JAK1 inhibitor treatment downregulated the β4 subunit mRNA levels significantly, with the treatment group having an expression level 50% lesser than that of the control group (Figure 2.13C).

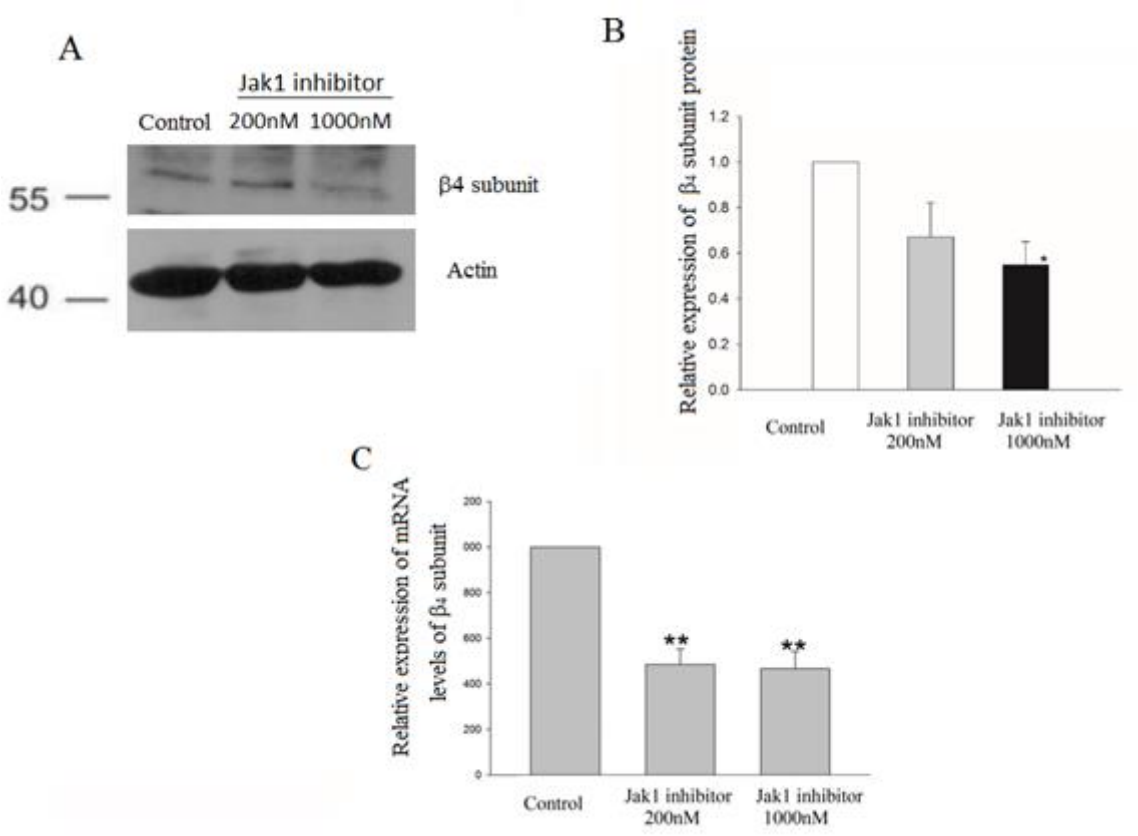

Figure 2.13: JAK1 inhibitor treatment reduces the expression of β4 subunit in H9c2 cells. Blots show β4 subunit (upper panel) and actin (lower panel) bands from whole cell fractions (A) of H9c2cells. Cells were untreated or treated with JAK1 inhibitor (GLPG0634) at concentrations of 200nM and 1000nM for 48 hrs. Relative expression of the β4 subunit from untreated or inhibitor treated cells are shown in bars (B). qRT-PCR analysis of relative expression of β4 mRNA of untreated and JAK1 inhibitor treated cells at concentrations of

200nm and 1000nm for 48hrs are shown in bars (C). All data are reported as mean values ± SD, *n* = 3-5 per group. *p < .05, **p < .01.

3.4.8 β_4 subunit promoter contains ISRE and GAS elements

The hypothesis that interferon β regulates the expression of the β_4 subunit was further strengthened by analysing the promoter region of the β_4 subunit gene. Specifically, we analysed the promoter sequence of rat β_4 subunit from 1000 bp 5' flanking region upstream from the first exon. In mammals, IFN inducible promoters contain a conserved sequence designated ISRE, and GAAA/TTTC motifs are also found in the promoter region of all IFN inducible genes. Sequence analysis of the promoter region revealed one putative ISRE element with a core sequence AAGTGA (Sheikh, Kobayashi, Matsuoka, Onyiah, & Plevy, 2011), at positions -836 to -846 and 9 GAAA/TTTC motifs oriented in both directions (Figure 2.14). In addition, we found from −286 to −295, a putative GAS element that matches the consensus sequence of (TTNCNNNAA) (Tessitore et al., 1998) which is known to be present in the promoters of mammalian IFN-γ responsive genes.

Figure 2.14: Promoter sequence of cacnb4 gene. The 5_UTR and promoter region is shown in bold capital letters. The 5_UTR intron region is indicated with italics. One ISRE site and one GAS site are shaded in grey. Nine GAAA/TTTC motifs are underlined. First exon indicated in italics (http://gpminer.mbc.nctu.edu.tw/).

3.4.9 Poly (I:C) and dengue virus increase the levels of intracellular Ca^{2+}

To test the possibility that the levels of cytosolic Ca^{2+} are increased by Poly (I:C) and DENV infection, fura 2 fluorescence determinations were performed in intact H9c2 cells, mock transfected (control) or transfected with Poly (I:C). Figure 2.15 summarizes results from several experiments. Figure 2.15B shows the average values of 340/380 nm fluorescence ratios as a function of time from control experiments (o) and from Poly (I:C) transfected cells (●). The dotted line indicates mean values under control and poly (I:C) conditions.

There was a significant increase in Ca^{2+} levels in resting Ca^{2+} by Poly (I:C) when compared to controls. A similar conclusion was reached when DENV2 infected cells were analysed. Infection brought about a significant increase in cytosolic Ca^{2+} (Fig. 2.15A). To determine whether an electrical stimulation has any effect on intracellular Ca^{2+} levels in Poly (I:C) transfected cells or in cells infected with the dengue virus, similar experiments were done, but results were not significantly different (results were not shown).

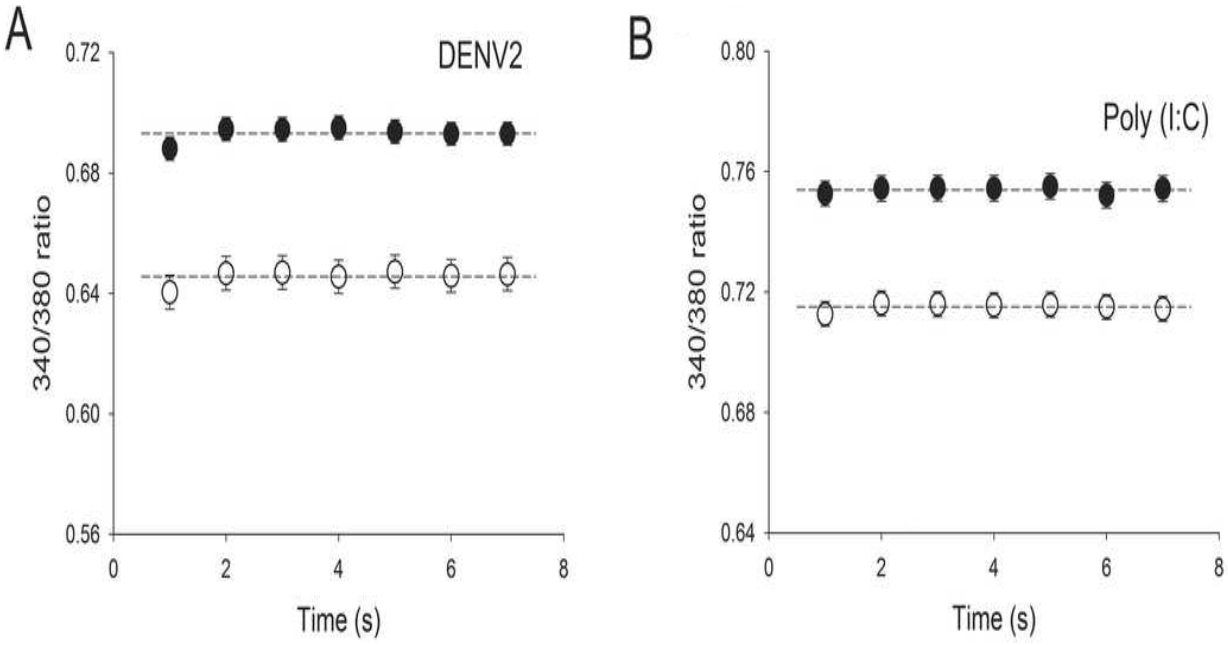

Figure 2.15: Effects DENV2 infection and poly (I:C) treatment on cytosolic Ca2+ measured 340/380 Fura 2 fluorescence. (A) Relationship between $[Ca^{2+}]_i$ and time in mock-infected (open symbols, n = 191) and in DENV2- infected H9c2 cells at 48-h postinfection (MOI = 5), (filled symbols, n = 187). (B) Relationship between $[Ca^{2+}]_i$ and time in H9c2 cells. Open symbols: empty vector-transfected cells (n = 453). Filled symbols: poly(I:C) 100-ng/ml transfected cells (n = 276). Average values for each condition are shown with dotted lines in A and B. All values are group means ± SEMs. *p < .01.

4. Discussion

In this study we demonstrated for the first time that the β_4 subunit of Cav1.2 channels can act as an antiviral agent. We found that β_4 subunit is localized both in nucleus and cytoplasm under both native and overexpressed conditions. Most importantly, overexpression of β_4 subunit enhanced the expression of four key antiviral proteins, namely: Ddx58, Irf7, stat2

and Ifitm3. Furthermore, β_4 subunit expression and nuclear translocation were increased when cells were challenged with DENV infection or transfected with poly (I:C), a synthetic analogue of double-stranded viral RNA (Field et al., 1967). Expression was also increased by IFNβ. In addition, we also observed both ISRE and GAS promoter elements in the promoter region of the β_4 subunit. Finally, we found that increasing β_4 subunit levels resulted in reduced expression of the non-structural DENV viral proteins NS1 and NS3 as well as a marked reduction in the number of DENV infected cells.

Our results are consistent with previous work in CD4 T-cells showing defective proliferation in the absence of β_4 subunit and reduced production of effector T-cell IFNγ levels in β_4 subunit -deficient CD4 T cells (Badou et al., 2006). Taken together, the present findings provide evidence in support of the hypothesis that the β_4 subunit plays a role in the response to infection.

Dengue infection in Heart

There are reports of patients with acute heart failure during DENV infection, and although cardiac impairment is not commonly reported, it can be life threatening. In fact, cases of complicated DENV infection with myocarditis have been described (Salgado et al., 2010; Marques et al., 2013; Zhang et al., 2010). Under this perspective and given the importance of myocardial lesion in severe dengue pathogenesis, we evaluated the susceptibility of the myoblast cell line H9c2, to DENV infection. This cell line, obtained from embryonic rat heart, represents a useful experimental model for cardiac cells because it is genetic homogeneous, its ease to grow and it is susceptibility to be genetically manipulated (Mejia-alvarez et al., 1994).

Initially, we demonstrated by the presence of the non-structural protein NS3 in the extracts from infected cells, that H9c2 cells are infected by the four DENV serotypes. While DENV2, DENV3 and DENV4 used in the assays were prototype strains, the DENV1 used in these assays corresponds to a DENV1 strain recently isolated from an infected human in Yucatán, México. At an MOI of 1, approximately 15% of the cells were infected after 24 h of infection. Moreover, the expression of structural and nonstructural viral proteins could be detected by confocal microscopy in DENV2 and DENV4 infected cells (Angel-Ambrocio et al., 2015).

Infection stimulates IFN-JAK-STAT pathway in H9c2 cells

Poly (I:C) is a double-stranded RNA (dsRNA) that signals through RIG-I/MDA5 mediating an intracellular dsRNA-activated antiviral pathway or through TLR3 mediating an extracellular dsRNA-activated antiviral pathway. Both recognition systems activate IRF3/IRF7 and NF-kB which, in turn, translocate to the nucleus and initiate the transcription of IFN-β gene. IFN-β then participates in an autocrine/paracrine loop by the JAK-STAT pathway, to activate the expression of later phase Interferon stimulating genes, including IRF7 that contributes to the positive-feedback regulation for the robust IFN production and is responsible for the late phase of IFN gene induction(Tamura et al., 2008). Our study also demonstrates that poly (I:C) induces production of IFN-β in H9c2 cells, suggesting that the same mechanism that operates in non-excitable cells is also present in cardiomiocytes. The β_4 subunit promoter has binding sites for IRF and STAT, and therefore it may be activated by Poly (I:C) and IFN. Notably, in mammals IRF7 is now highlighted as the "master regulator" in IFN production via TLR 7/9-MyD88-dependent signaling pathway, and the formation of a heterodimer between IRF7 and IRF3, rather than an IRF3 homodimer, is presumed to be crucial for the production of early phase of IFN during virus infection (Honda et al., 2005).

β_4 subunit expression is regulated by IFN-JAK-STAT pathway

Immunoblot and immunofluorescence analysis showed a significant upregulation of β_4 subunit protein upon DENV infection or poly (I:C) treatment. Consistent with the hypothesis that an intermediate upregulates β_4 subunit in H9C2 cells, possibly interferon when cells are infected by DENV infected cells or transfected with poly (I:C), our study showed a significant induction of β_4 subunit when cells were treated with supernatants that contain soluble factors released during DENV infection or after treatment with Ifnb. These results highlight a significant role of β_4 subunit during the antiviral immune response.

As demosntrated in the present work, the expression of the β_4 subunit is regulated by IFN-JAK-STAT pathway. The involvement of JAK-STAT pathway could be demonstrated by studying the expression of β_4 subunit in cells treated with the selective JAK1 inhibitor GLPG0634. The inhibitor interferes with JAK1 protein and further prevents activation of

STAT factors. The activated form of STAT is directly involved in upregulation of Interferon stimulating genes. Our RT-PCR and western blot analysis confirmed a significant down regulation of β_4 subunit upon JAK1 inhibitor treatment, suggesting that JAK1 and its downstream signaling pathway plays a crucial role in regulating the expression of β_4 subunit.

The responsiveness of β_4 subunit to IFN was further confirmed by analysis of its promoter region. The structure of the rat β_4 subunit promoter possesses a typical organization of the promoter of IFN inducible genes. Thus, ISRE and GAS motifs exist in the promoter region. The β_4 subunit promoter has one ISRE motif at the position of -846 to -836 and one GAS element in the range of -295 to -286 nucleotide position near to transcriptional start site. Functional studies of the β_4 subunit promoter are required to elucidate in detail the molecular mechanisms involved but these experiments are beyond the scope of the present thesis.

Role of Intracellular Calcium

The β_4 subunit is associated with the trafficking of the α1c subunit, the principal subunit of the Cav1.2 channels to the plasma membrane in excitable cells (Dolphin, 2003). When bound to the α1c subunit, it regulates the kinetic properties of Ca^{2+} currents flowing through these channels increasing the open probability of the channel and shifting the activation curve towards more negative potentials (Colecraft et al., 2002; Hullin et al., 2003; Neely et al., 1993). The effects of the β_4 subunit on antiviral factor production demonstrated in the present work are likely independent of its involvement in regulating channel gating properties and trafficking given that these functions involve interactions with the α1c subunit at the cell membrane, not in the nucleus where expression of genes is affected.

Although the cellular mechanisms that underlie the triggering of nuclear translocation of β_4 subunit following DENV infection or poly (I:C) treatment or IFNb treatment and the increased expression of IFN-related genes in response to β_4 subunit expression remain to be resolved, it is reasonable to postulate that intracellular Ca^{2+} could play a role in these processes. Human skeletal myotubes from DENV-infected patients had elevated resting levels of Ca^{2+}, as measured with ion-sensitive microelectrodes (Salgado et al., 2010), consistent with intracellular Ca^{2+} playing a role in the dengue fever pathogenesis. Additionally, Tadmouri et al. (2012) found that β_4 subunit-mediated repression of tyrosine hydroxylase mRNA expression and β_4 subunit translocation to the nucleus of hippocampal neurons depend on electrical activity. In hippocampal neurons, electrical activity associated

with action potentials is accompanied by transient elevations in cytosolic Ca^{2+} that are controlled in part by a Ca^{2+}-induced Ca^{2+} release mechanism, similar to that in heart muscle (Sandler & Barbara, 1999). A relationship between β_4 subunit and intracellular Ca^{2+} has also been found in immune cells. Moreover, Badou et al. (2006) described that β_4 subunit -deficient T cells have abnormally low Ca^{2+} responses when stimulated as well as reduced cytokine IFNγ production and impaired nuclear translocation of NFAT (nuclear factor of activated T cells) following stimulation. A connection between IFNγ and intracellular Ca^{2+} levels was reported in human microglia, the phagocytic cells of the brain. Franciosi et al. reported that the acute application of IFNγ induces an immediate, progressive increase in Ca^{2+} to a plateau level in human microglia (Franciosi et al., 2002).

In T cells, the influx of Ca^{2+} associated with stimulation occurs through voltage-independent Ca^{2+} channels (Badou et al., 2006). In the present experiments, the source of Ca^{2+} flowing into the cytosol is unknown and could be extracellular via Ca^{2+}-permeant cell membrane channels. However, the Cav1.2 channel is an unlikely candidate because the H9c2 cells used in these experiments show very little excitability and measurable Ca^{2+} currents can only be recorded after several weeks in culture (Hescheler et al., 1991). Furthermore, although resting $[Ca^{2+}]_i$ increased by DENV infection or by Poly(I:C), we did not observe a further rise in cytosolic Ca^{2+} in our cells following electrical stimulation.

β_4 subunit involved in regulating gene transcription

The four known β subunits (β_1, β_2, β_3, and β_4) have different distributions in the cell (Colecraft et al., 2002; Foell et al., 2004). β_4 subunit is the only one for which a predominant presence in cardiomyocyte nuclei has been described; this observation was reported by Colecraft et al. (Colecraft et al., 2002) in rat cardiomyocytes following recombinant adenoviral gene infection used to overexpress green fluorescent protein-fused β_4 subunit. On the other hand, Foell et al. (2004) observed native β_4 subunit expression in the cell membrane of canine cardiomyocytes. The differing findings between these studies could be related to a species difference. Alternatively, the observation of Colecraft and colleagues could have reflected nuclear translocation of β_4 subunit in response to adenoviral-infection, similar to the postinfection translocation effects observed in the present study. It should be noted, however, that we observed native β_4 subunit expression in both cytoplasmic and nuclear fractions of H9c2 cells. Moreover, when β_4 subunit was overexpressed, its abundance was

increased in both fractions, suggesting that the transfection itself did not have a major effect on the cellular distribution of β_4 subunit.

The β_4 subunit has been related to transcription in non-cardiac cells previously. Hibino et al. (2003) found that β_{4c}, a short form of the subunit predominantly expressed in cochlear cells, is recruited to the nucleus and interacts directly with the chromo shadow domain of chromobox protein2/heterochromatin protein 1γ, a nuclear protein involved in gene silencing and transcriptional regulation. The β_4-chromo shadow domain interaction reduced the silencing activity of this chromobox protein dramatically in Cos1 cells. Tadmouri et al. (2012) found that β_4 subunit localizes predominantly in the nuclei of dentate gyrus neurons and, using a heterologous expression system, showed that it associates with Ppp2r5d, a regulatory subunit of PP2A phosphatase, followed by nuclear translocation of the complex thus enabling repression of the tyrosine hydroxylase gene promoter by the β_4 subunit. They proposed that β_4 subunit might act as a repressor recruiting platform to control neuronal gene expression. These two examples demonstrate modulatory actions of β_4 subunit on repressive gene phenomena that are distinct from its stimulatory effects on antiviral factor expression reported here, and thus likely mediated by different targets.

Interferons possibly mediates β_4 subunit induced antiviral factors

The increased expression of IFNb1 following β_4 subunit overexpression demonstrated in this study is consistent with the possibility that β_4 subunit-mediated upregulation of antiviral factors may involve IFNs. IFNs are known stimulators of the expression of the antiviral factors Ddx58, Irf7, and Ifitm3 (Schoggins & Rice, 2011) and have been shown previously to induce Ifitm3 expression in H9c2 cells (Lau et al., 2012). These potent antiviral factors reinforce the system by inducing further upregulation of IFN levels. A knockout mouse study described that Irf7 is necessary for induction of IFN-α/β (Honda et al., 2005). When Ddx58 interacts with double-stranded RNA (a replication intermediate for RNA viruses), a signalling cascade is triggered, leading to activation of transcription factors and induction of IFNs (Yoneyama et al., 2004).

The suggested role of IFNs in β_4 subunit-mediated upregulation of antiviral factors is supported by the fact that β_4 subunit-upregulated antiviral factors play important roles during DENV infection. IFN receptor-deficient mice are highly susceptible to DENV infection (Johnson & Roehrig, 1999). Meanwhile, Ddx58, Irf7 and Iftim3 significantly reduce DENV

replication; in particular, Ifitm3 targets DENV at an early life-cycle stage (Schoggins et al., 2012). Diffusion of IFN (or another soluble factor) may explain our present observation of increased β_4 subunit expression and nuclear translocation in non-infected cells near DENV-infected cells.

Given that Ddx58, Irf7, and Ifitm3 are important antiviral factors in many cell types against a variety of viruses (Hoffmann et al., 2015), we expect that the anti-DENV protective effects of β_4 subunit demonstrated here may extend to other viruses and other differentiated cell types. Our results with poly (I:C) are consistent with this assumption. β_4 subunit is expressed in excitable cells, including neurons in diverse brain regions (Ludwig et al., 1997) and cardiomyocytes (Foell, 2004), as well as in non-excitable cells, including T cells (Stokes et al., 2004) and cells in the kidney and testis (Escayg et al., 1998). Of the four β_4 subunit isoforms (a-d) that have been described associated to Cav1.2 channels (A. Rohrkasten et al., 1989; Lacerda et al., 1991; Singer et al., 1991), three are expressed in heart, namely a, b, and d (Foell, 2004). The β_{4d} isoform (not recognized by the β_4 subunit antibody used here) is truncated due to a frame-shift mediated early stop codon, resulting in an absence of the domain that interacts strongly with the α1c subunit (Foell, 2004). The physiological relevance of β_{4d} is unknown. The remaining β_4 subunit (β_{4a} and β_{4b}) have similar molecular weights and could not be distinguished from one another in our immunoblots. However, β_{4b} subunit has been shown to have a greater nuclear targeting and gene regulatory effects than β_{4a} subunit in cultured cerebellar granule cells (Etemad et al., 2014), suggesting it may have a preferential role in gene regulation. Our findings that β_{4b} subunit transfection led to a preferential nuclear location and upregulation of IFN-related genes are consistent with this view.

In conclusion, our experiments suggest that the β_4 subunit of Cav1.2 channels in H9c2 cells plays a crucial role in the cellular response to infection with DENV. This cellular response involves upregulation of key antiviral proteins and represents a novel role of this calcium channel subunit in heart.

5. Conclusions

- Under β_4 overexpressed and endogenous conditions, β_4 is localized in nucleus and cytosolic fractions of H9c2 cells.
- β_4 subunit overexpression enhances expression of interferon related factors and reduces dengue virus infection levels.
- Viral infection enhances β_4 subunit expression particularly in sites of infection.
- β_4 subunit expression is regulated by interferon IFN-JAK-STAT pathway.

6. Publications

Part of the thesis work discussed in this dissertation was published in one publication and most of the work is under preparation of another manuscript.

1) Angel-Ambrocio, A. H., Soto-Acosta, R., **Tammineni, E. R**., Carrillo, E. D., Bautista-Carbajal, P., Hernández, A., … del Angel, R. M. (2015). An embryonic heart cell line is susceptible to dengue virus infection. *Virus Research, 198*, 53–58. http://doi.org/10.1016/j.virusres.2015.01.004

2) Eshwar R Tammineni, Elba D Carrillo, Rubén Soto-Acosta, Antonio H Angel-Ambrocio, Maria C García, Patricia Bautista-Carbajal, Rosa M del Angel, Jorge Alberto Sanchez. **The β4 Subunit of Cav1.2 channels in cardiac cells upregulates interferon-related genes and inhibits denguevirus infection.** *Manuscript under preparation.*

7. References

A. ROHRKASTEN, w. N., H. E. MEYER, M. SIEBER, T. S., & ST. REGULLA, A. F. H. (1989). Identification of the CAMP-Specific Phosphorylation Site of the Purified Skeletal Muscle Receptor for. *Annals of the New York Academy of Sciences*, *697*.

Agarwal, R., Kapoor, S., Nagar, R., Misra, a K., Tandon, R., Mathur, a, … Chaturvedi, U. C. (1999). A clinical study of the patients with dengue hemorrhagic fever during the epidemic of 1996 at Lucknow, India. *Southeast Asian Journal of Tropical Medicine and Public Health*. Retrieved from <Go to ISI>://BCI:BCI200000326429

Akira, S., Uematsu, S., & Takeuchi, O. (2006). Pathogen recognition and innate immunity. *Cell*, *124*(4), 783–801. http://doi.org/10.1016/j.cell.2006.02.015

Angel-Ambrocio, A. H., Soto-Acosta, R., Tammineni, E. R., Carrillo, E. D., Bautista-Carbajal, P., Hernández, A., … del Angel, R. M. (2015). An embryonic heart cell line is susceptible to dengue virus infection. *Virus Research*, *198*, 53–58. http://doi.org/10.1016/j.virusres.2015.01.004

Badou, A., Jha, M. K., Matza, D., Mehal, W. Z., Freichel, M., Flockerzi, V., & Flavell, R. a. (2006). Critical role for the beta regulatory subunits of Cav channels in T lymphocyte function. *Proceedings of the National Academy of Sciences of the United States of America*, *103*(42), 15529–15534. http://doi.org/10.1073/pnas.0607262103

Barbalat, R., Lau, L., Locksley, R. M., & Barton, G. M. (2009). Toll-like receptor 2 on inflammatory monocytes induces type I interferon in response to viral but not bacterial ligands. *Nature Immunology*, *10*(11), 1200–1207. http://doi.org/10.1038/ni.1792

Buraei, Z., & Yang, J. (2010). The ß subunit of voltage-gated Ca2+ channels. *Physiological Reviews*, *90*(4), 1461–1506. http://doi.org/10.1152/physrev.00057.2009.

Buraei, Z., & Yang, J. (2013). Structure and function of the β subunit of voltage-gated Ca2+ channels. *Biochimica et Biophysica Acta (BBA) - Biomembranes*, *1828*(7), 1530–1540. http://doi.org/10.1016/j.bbamem.2012.08.028

Burgess, D. L., Jones, J. M., Meisler, M. H., & Noebels, J. L. (1997). Mutation of the Ca2+ Channel β Subunit Gene Cchb4 Is Associated with Ataxia and Seizures in the Lethargic (lh) Mouse. *Cell*, *88*(3), 385–392. http://doi.org/10.1016/S0092-8674(00)81877-2

Cabral, M. D., Paulet, P.-E., Robert, V., Gomes, B., Renoud, M.-L., Savignac, M., … Pelletier, L. (2010). Knocking Down Ca_v1 Calcium Channels Implicated in Th2 Cell Activation Prevents Experimental Asthma. *American Journal of Respiratory and Critical Care Medicine*, *181*(12), 1310–1317. http://doi.org/10.1164/rccm.200907-1166OC

Carbone, E., & Lux, H. D. (1987). Single low-voltage-activated calcium channels in chick and rat sensory neurones. *The Journal of Physiology*, *386*, 571–601.

Castellano, a, Wei, X., Birnbaumer, L., & Perez-Reyes, E. (1993). Cloning and expression of a neuronal calcium channel beta subunit. *The Journal of Biological Chemistry*, *268*(17), 12359–12366.

Catterall, W. a. (2000). S Tructure and R Egulation of.

Catterall, W. a, Perez-Reyes, E., Snutch, T. P., & Striessnig, J. (2005). International Union of Pharmacology. XLVIII. Nomenclature and structure-function relationships of voltage-gated calcium channels. *Pharmacological Reviews*, *57*(4), 411–425. http://doi.org/10.1124/pr.57.4.5.units

Chaturvedi, U. C., Elbishbishi, E. a., Agarwal, R., Raghupathy, R., Nagar, R., Tandon, R., … Azizieh, F. (1999). Sequential production of cytokines by dengue virus-infected human peripheral blood leukocyte cultures. *Journal of Medical Virology*, *59*(3), 335–340. http://doi.org/10.1002/(SICI)1096-9071(199911)59:3<335::AID-JMV13>3.0.CO;2-E

Chen, Y., Li, M., Zhang, Y., Lin-ling, H., Yamada, Y., Fitzmaurice, A., … Yang, J. (2004). Structural basis of the a1 – b subunit interaction of voltage-gated Ca channels. *Nature*, *429*(June), 675–680. http://doi.org/10.1038/nature02588.Published

Colecraft, H. M., Alseikhan, B., Takahashi, S. X., Chaudhuri, D., Mittman, S., Yegnasubramanian, V., … Yue, D. T. (2002). Novel functional properties of Ca $^{2+}$ channel β subunits revealed by their expression in adult rat heart cells. *The Journal of Physiology*, *541*(2), 435–452. http://doi.org/10.1113/jphysiol.2002.018515

De Waard, M., Pragnell, M., & Campbell, K. P. (1994). Ca2+ channel regulation by a conserved beta subunit domain. *Neuron*, *13*, 495–503. http://doi.org/10.1016/0896-6273(94)90363-8

Dolphin, A. C. (2003). β Subunits of Voltage-Gated Calcium Channels, *35*(6).

Doris Martha Salgado, M., , José Miguel Eltit, PhD, Keith Mansfield, DVM, C., Panqueba, M., , Dolly Castro, M., & , Martha Rocio Vega, M. (2010). NIH Public Access. *Journal of Infectious Diseases, The*, *29*(3), 238–242. http://doi.org/10.1097/INF.0b013e3181bc3c5b.Heart

Eissenberg, J. C., James, T. C., Foster-Hartnett, D. M., Hartnett, T., Ngan, V., & Elgin, S. C. (1990). Mutation in a heterochromatin-specific chromosomal protein is associated with suppression of position-effect variegation in Drosophila melanogaster. *Proceedings of the National Academy of Sciences of the United States of America*, *87*(24), 9923–9927. http://doi.org/10.1073/pnas.87.24.9923

Ellinor, P. T., Zhang, J. F., Randall, a D., Zhou, M., Schwarz, T. L., Tsien, R. W., & Horne, W. a. (1993). Functional expression of a rapidly inactivating neuronal calcium channel. *Nature*, *363*(6428), 455–458. http://doi.org/10.1038/363455a0

Escayg, a, Jones, J. M., Kearney, J. a, Hitchcock, P. F., & Meisler, M. H. (1998). Calcium channel beta 4 (CACNB4): human ortholog of the mouse epilepsy gene lethargic. *Genomics*, *50*(50), 14–22. http://doi.org/10.1006/geno.1998.5311

Etemad, S., Obermair, G. J., Bindreither, D., Benedetti, A., Stanika, R., Di Biase, V., … Flucher, B. E. (2014). Differential neuronal targeting of a new and two known calcium channel β4 subunit splice variants correlates with their regulation of gene expression. *The Journal of Neuroscience : The Official Journal of the Society for Neuroscience*, *34*(4), 1446–61. http://doi.org/10.1523/JNEUROSCI.3935-13.2014

Farid Uddin Ahmed*, Chowdhury B Mahmood, J. D. S., Syed Mesbahul Hoque, R. Z. and M. S. H., & Department of Paediatrics, Chittagong Medical College, Chittagong-4000, B. (2001). Dengue and Dengue Haemorrhagic Fever in Children During the 2000 Outbreak in Chittagong, Bangladesh. *Dengue Bulletin*, *25*(December), 1–136.

Field, a K., Tytell, a a, Lampson, G. P., & Hilleman, M. R. (1967). Inducers of interferon and host resistance. II. Multistranded synthetic polynucleotide complexes. *Proceedings of the National Academy of Sciences of the United States of America*, *58*(3), 1004–10. http://doi.org/10.1073/pnas.58.3.1004

Fitzgerald, K. a., McWhirter, S. M., Faia, K. L., Rowe, D. C., Latz, E., Golenbock, D. T., … Maniatis, T. (2003). IKKε and TBK1 are essential components of the IRF3 signaling pathway. *Nature Immunology*, *4*(5), 491–496. http://doi.org/10.1038/ni921

Foell, J. D. (2004). Molecular heterogeneity of calcium channel -subunits in canine and human heart: evidence for differential subcellular localization. *Physiological Genomics*, *17*(2), 183–200. http://doi.org/10.1152/physiolgenomics.00207.2003

Foell, J. D., Balijepalli, R. C., Delisle, B. P., Yunker, A. M. R., Robia, S. L., Walker, J. W., … Kamp, T. J. (2004). Molecular heterogeneity of calcium channel beta-subunits in canine and human heart: evidence for differential subcellular localization. *Physiological Genomics*, *17*(2), 183–200. http://doi.org/10.1152/physiolgenomics.00207.2003

Franciosi, S., Choi, H. B., Kim, S. U., & McLarnon, J. G. (2002). Interferon-?? acutely induces calcium influx in human microglia. *Journal of Neuroscience Research*, *69*(August), 607–613. http://doi.org/10.1002/jnr.10331

Gomez-Ospina, N., Tsuruta, F., Barreto-Chang, O., Hu, L., & Dolmetsch, R. (2006). The C Terminus of the L-Type Voltage-Gated Calcium Channel CaV1.2 Encodes a Transcription Factor. *Cell*, *127*(3), 591–606. http://doi.org/10.1016/j.cell.2006.10.017

Gubler, D. J. (2004). The changing epidemiology of yellow fever and dengue, 1900 to 2003: Full circle? *Comparative Immunology, Microbiology and Infectious Diseases*, *27*, 319–330. http://doi.org/10.1016/j.cimid.2004.03.013

Guzmán, M. G., Alvarez, M., Rodríguez, R., Rosario, D., Vázquez, S., Valdés, L., … Kourí, G. (1999). Fatal dengue hemorrhagic fever in Cuba, 1997. *International Journal of Infectious Diseases*, *3*(3), 130–135. http://doi.org/10.1016/S1201-9712(99)90033-4

Guzmán, M. G., & Kouri, G. (2002). Dengue: an update. *The Lancet Infectious Diseases*, *2*(1), 33–42. http://doi.org/10.1016/S1473-3099(01)00171-2

Guzmán, M. G., & Kourí, G. (1996). Advances in dengue diagnosis. *Clinical and Diagnostic Laboratory Immunology*, *3*(6), 621–627.

Guzman, M. G., Kouri, G. P., Bravo, J., Soler, M., Vazquez, S., Santos, M., … Ballester, J. M. (1984). Dengue Hemorrhagic-Fever in Cuba .2. Clinical Investigations. *Transactions of the Royal Society of Tropical Medicine and Hygiene*, *78*(0), 239–241. http://doi.org/10.1016/0035-9203(84)90286-4

Helton, T. D., Kojetin, D. J., Cavanagh, J., & Horne, W. a. (2002). Alternative splicing of a beta4 subunit proline-rich motif regulates voltage-dependent gating and toxin block of Cav2.1 Ca2+ channels. *The Journal of Neuroscience : The Official Journal of the Society for Neuroscience*, *22*(21), 9331–9339.

Hescheler, J., Meyer, R., Plant, S., Krautwurst, D., Rosenthal, W., & Schultz, G. (1991). Morphological, biochemical, and electrophysiological characterization of a clonal cell (H9c2) line from rat heart. *Circulation Research*, *69*, 1476–1486. http://doi.org/10.1161/01.RES.69.6.1476

Hibino, H., Pironkova, R., Onwumere, O., Rousset, M., Charnet, P., Hudspeth, a J., & Lesage, F. (2003). Direct interaction with a nuclear protein and regulation of gene silencing by a variant of the Ca2+-channel beta 4 subunit. *Proceedings of the National Academy of Sciences of the United States of America*, *100*(1), 307–312. http://doi.org/10.1073/pnas.0136791100

Hoffmann, H. H., Schneider, W. M., & Rice, C. M. (2015). Interferons and viruses: An evolutionary arms race of molecular interactions. *Trends in Immunology*, *36*(3), 124–138. http://doi.org/10.1016/j.it.2015.01.004

Honda, K., Takaoka, A., & Taniguchi, T. (2006). Type I Inteferon Gene Induction by the Interferon Regulatory Factor Family of Transcription Factors. *Immunity*, *25*(3), 349–360. http://doi.org/10.1016/j.immuni.2006.08.009

Honda, K., Yanai, H., Negishi, H., Asagiri, M., Sato, M., Mizutani, T., … Taniguchi, N. Y. & T. (2005). IRF-7 is the master regulator of. *Nature*, *434*(April), 772–777. http://doi.org/10.1038/nature03419.1.

Hongsiriwon, S. (2002). Dengue hemorrhagic fever in infants. *The Southeast Asian Journal of Tropical Medicine and Public Health*, *33*(1), 49–55. Retrieved from http://www.ncbi.nlm.nih.gov/pubmed/12118460

Hullin, R., Khan, I. F. Y., Wirtz, S., Mohacsi, P., Varadi, G., Schwartz, A., & Herzig, S. (2003). Cardiac L-type calcium channel beta-subunits expressed in human heart have differential effects on single channel characteristics. *The Journal of Biological Chemistry*, *278*(24), 21623–21630. http://doi.org/10.1074/jbc.M211164200

Jha, M. K., Badou, A., Meissner, M., McRory, J. E., Freichel, M., Flockerzi, V., & Flavell, R. a. (2009). Defective survival of naive CD8+ T lymphocytes in the absence of the β3 regulatory subunit of voltage-gated calcium channels. *Nature Immunology*, *10*(12), 1275–1282. http://doi.org/10.1038/ni.1793

Johnson, a J., & Roehrig, J. T. (1999). New mouse model for dengue virus vaccine testing. *Journal of Virology*, *73*(1), 783–786.

Kabra, S. K., Verma, I. C., Arora, N. K., Jain, Y., & Kalra, V. (1992). Dengue haemorrhagic fever in children in Delhi. *Bull World Health Organ*, *70*(1), 105–108.

Kabra, S. K., Y. Jain, R. M. Pandey, Madhulika, T. Singhal, P. Tripathi, S. Broog, P. S. and, & Seth, V. (1999). Dengue haemorrhagic fever in children in the 1996 Delhi epidemic. *Trans R Soc Trop Med Hyg*, *93*, 294–298.

Kalayanarooj S, Nimmannitya S, S. S. (1999). Can doctors make an accurate diagnosis of dengue infections at an early stage. *Dengue Bulletin*, *23*, 1–9.

Kawai, T., Takahashi, K., Sato, S., Coban, C., Kumar, H., Kato, H., … Akira, S. (2005). IPS-1, an adaptor triggering RIG-I- and Mda5-mediated type I interferon induction. *Nat Immunol*, *6*(10), 981–988. http://doi.org/10.1038/ni1243

Lacerda, a E., Kim, H. S., Ruth, P., Perez-Reyes, E., Flockerzi, V., Hofmann, F., … Brown, a M. (1991). Normalization of current kinetics by interaction between the alpha 1 and beta subunits of the skeletal muscle dihydropyridine-sensitive Ca2+ channel. *Nature*. http://doi.org/10.1038/352527a0

Lau, S. L. Y., Yuen, M. L., Kou, C. Y. C., Au, K. W., Zhou, J., & Tsui, S. K. W. (2012). Interferons induce the expression of IFITM1 and IFITM3 and suppress the proliferation of rat neonatal cardiomyocytes. *Journal of Cellular Biochemistry*, *113*(3), 841–847. http://doi.org/10.1002/jcb.23412

Lavanya, M., Cuevas, C. D., Thomas, M., Cherry, S., & Ross, S. R. (2013). siRNA Screen for Genes That Affect Junin Virus Entry Uncovers Voltage-Gated Calcium Channels as a Therapeutic Target. *Science Translational Medicine*, *5*(204), 204ra131–204ra131. http://doi.org/10.1126/scitranslmed.3006827

Leslie T. Cooper. (2009). Myocarditis. *N Engl J Med*, *360*, 1526–1538.

Libraty, D. H., Young, P. R., Pickering, D., Endy, T. P., Kalayanarooj, S., Green, S., … Rothman, A. L. (2002). High circulating levels of the dengue virus nonstructural protein NS1 early in dengue illness correlate with the development of dengue hemorrhagic fever. *The Journal of Infectious Diseases*, *186*(8), 1165–1168. http://doi.org/10.1086/343813

Lu, L., Sirish, P., Zhang, Z., Woltz, R. L., Li, N., Timofeyev, V., … Chiamvimonvat, N. (2015). Regulation of Gene Transcription by Voltage-gated L-type Calcium Channel, $Ca_v1.3$. *Journal of Biological Chemistry*, *290*(8), 4663–4676. http://doi.org/10.1074/jbc.M114.586883

Ludwig, a, Flockerzi, V., & Hofmann, F. (1997). Regional expression and cellular localization of the alpha1 and beta subunit of high voltage-activated calcium channels in rat brain. *The Journal of Neuroscience : The Official Journal of the Society for Neuroscience*, *17*(4), 1339–1349.

Marques, N., Gan, V. C., & Leo, Y.-S. (2013). Dengue myocarditis in Singapore: two case reports. *Infection*, *41*(3), 709–14. http://doi.org/10.1007/s15010-012-0392-9

Medzhitov, R. (2007). Recognition of microorganisms and activation of the immune response. *Nature*, *449*(7164), 819–826. http://doi.org/10.1038/nature06246

MEJIA-ALVAREZ, R., TOMASELLI, G. F., & MARBAN, E. (n.d.). SIMULTANEOUS EXPRESSION OF CARDIAC AND SKELETAL MUSCLE ISOFORMS OF THE L-TYPE CA2+ CHANNEL IN A RAT HEART MUSCLE CELL LINE . *Journal of Physiology*, *478*(2), 315–329. Retrieved from http://cat.inist.fr/?aModele=afficheN&cpsidt=11234002

Mermelstein, P. G., Deisseroth, K., Dasgupta, N., Isaksen, a L., & Tsien, R. W. (2001). Calmodulin priming: nuclear translocation of a calmodulin complex and the memory of prior neuronal activity. *Proceedings of the National Academy of Sciences of the United States of America*, *98*(26), 15342–15347. http://doi.org/10.1073/pnas.211563998

Mikami, A., Imoto, K., Tanabe, T., & Niidome, T. (1989). Primary structure and functional expression of the cardiac dihydropyridine-sensitive calcium channel. *Nature*, *340*, 230–233. Retrieved from http://www.nature.com/nature/journal/v340/n6230/abs/340230a0.html

Miller, Kristin A., Siscovick D.S., Sheppard L., Shepherd K., Sullivan, J. H., Anderson, G. L., Ph, D., & Kaufman, J. D. (2007). New England Journal, 119–130.

Morgan, J. I., & Curran, T. (1986). Role of ion flux in the control of c-fos expression. *Nature*, *322*(6079), 552–5. http://doi.org/10.1038/322552a0

Morrison, D. G. (1984). TUMOR GROWTH RATE VARIES WITH AGE IN LETHARGIC MUTANT BALB/cGnDu MICE. *Developmental and Comparative Immunology*, *8*(2), 435–442. http://doi.org/10.1017/CBO9781107415324.004

Mustafa, a. S., Elbishbishi, E. a., Agarwal, R., & Chaturvedi, U. C. (2001). Elevated levels of interleukin-13 and IL-18 in patients with dengue hemorrhagic fever. *FEMS Immunology and Medical Microbiology*, *30*(3), 229–233. http://doi.org/10.1016/S0928-8244(01)00227-9

Neely, A., Wei, X., Olcese, R., Birnbaumer, L., & Stefani, E. (1993). Wei,t Riccardo. *Science*, *17*(June).

Nimmannitya, S. (2002). DENGUE HAEMORRHAGIC FEVER: CURRENT ISSUES AND FUTURE RESEARCH. *Asian-Oceanian Journal of Paediatrics and Child Health*, *1*, 1–21.

Obeyesekere, I., & Hermon, Y. (1973). Arbovirus heart disease: Myocarditis and cardiomyopathy following dengue and chikungunya fever-A follow-up study. *American Heart Journal*, *85*(2), 186–194. http://doi.org/10.1016/0002-8703(73)90459-6

Omilusik, K., Priatel, J. J., Chen, X., Wang, Y. T., Xu, H., Choi, K. B., … Jefferies, W. A. (2011). The CaV1.4 Calcium Channel Is a Critical Regulator of T Cell Receptor Signaling and Naive T Cell Homeostasis. *Immunity*, *35*(3), 349–360. http://doi.org/10.1016/j.immuni.2011.07.011

Platanias, L. C., & Lurie, R. H. (2005). MECHANISMS OF TYPE □ I □ AND TYPE □ II □ INTERFERON □ MEDIATED SIGNALLING, *5*(May), 375–386. http://doi.org/10.1038/nri1604

Richards, a L., Bagus, R., Baso, S. M., Follows, G. a, Tan, R., Graham, R. R., … Punjabi, N. (1997). The first reported outbreak of dengue hemorrhagic fever in Irian Jaya, Indonesia. *Am J Trop Med Hyg*, *57*(1), 49–55.

Rubio, N., Almanza, a, Mercado, F., Arévalo, M.-Á., Garcia-Segura, L. M., Vega, R., & Soto, E. (2013). Upregulation of voltage-gated Ca2+ channels in mouse astrocytes infected with Theiler's murine encephalomyelitis virus (TMEV). *Neuroscience*, *247*, 309–18. http://doi.org/10.1016/j.neuroscience.2013.05.049

Saha, S. K., Pietras, E. M., He, J. Q., Kang, J. R., Liu, S.-Y., Oganesyan, G., … Cheng, G. (2006). Regulation of antiviral responses by a direct and specific interaction between TRAF3 and Cardif. *The EMBO Journal*, *25*(14), 3257–63. http://doi.org/10.1038/sj.emboj.7601220

Salgado, D. M., Panqueba, C. a, Castro, D., & Vega, M. R. (2009). Miocarditis en Niños con Fiebre por Dengue Hemorrágico en un Hospital Universitario de Colombia. *Rev. Salud Pùblica*, *11*(October 2005), 591–600. http://doi.org/10.1590/S0124-00642009000400010

Sandler, V. M., & Barbara, J. G. (1999). Calcium-induced calcium release contributes to action potential-evoked calcium transients in hippocampal CA1 pyramidal neurons. *The Journal of Neuroscience : The Official Journal of the Society for Neuroscience*, *19*(11), 4325–4336.

Schoggins, J. W., Dorner, M., Feulner, M., Imanaka, N., Murphy, M. Y., Ploss, A., & Rice, C. M. (2012). Dengue reporter viruses reveal viral dynamics in interferon receptor-deficient mice and sensitivity to interferon effectors in vitro. *Proceedings of the National Academy of Sciences of the United States of America*, *109*(36), 14610–5. http://doi.org/10.1073/pnas.1212379109

Schoggins, J. W., & Rice, C. M. (2011). Interferon-stimulated genes and their antiviral effector functions. *Current Opinion in Virology*, *1*(6), 519–525. http://doi.org/10.1016/j.coviro.2011.10.008

Seth, R. B., Sun, L., Ea, C.-K., & Chen, Z. J. (2005). Identification and Characterization of MAVS, a Mitochondrial Antiviral Signaling Protein that Activates NF-κB and IRF3. *Cell*, *122*(5), 669–682. http://doi.org/10.1016/j.cell.2005.08.012

Sharma, S., tenOever, B. R., Grandvaux, N., Zhou, G. P., Lin, R., & Hiscott, J. (2003). Triggering the interferon antiviral response through an IKK-related pathway. *Science*, *300*(5622), 1148–1151. http://doi.org/10.1126/science.1081315\r1081315 [pii]

Sheikh, S. Z., Kobayashi, T., Matsuoka, K., Onyiah, J. C., & Plevy, S. E. (2011). Characterization of an interferon-stimulated response element (ISRE) in the Il23a promoter. *The Journal of Biological Chemistry*, *286*(2), 1174–80. http://doi.org/10.1074/jbc.M110.147884

Singer, D., Biel, M., Lotan, I., Flockerzi, V., Hofmann, F., & Dascal, N. (1991). The roles of the subunits in the function of the calcium channel. *Science*, *253*(5027), 1553–1557. http://doi.org/10.1126/science.1716787

Stokes, L., Gordon, J., & Grafton, G. (2004). Non-voltage-gated L-type Ca2+ channels in human T cells: Pharmacology and molecular characterization of the major α pore-forming and auxiliary β-subunits. *Journal of Biological Chemistry*, *279*(19), 19566–19573. http://doi.org/10.1074/jbc.M401481200

Subramanyam, P., Obermair, G. J., Baumgartner, S., Gebhart, M., Striessnig, J., Kaufmann, W. a, … Flucher, B. E. (2009). Activity and calcium regulate nuclear targeting of the calcium channel beta4b subunit in nerve and muscle cells. *Channels (Austin, Tex.)*, *3*(5), 343–55. Retrieved from http://www.ncbi.nlm.nih.gov/pmc/articles/PMC2853709/\nhttp://www.pubmedcentral.nih.gov/articlerender.fcgi?artid=2853709&tool=pmcentrez&rendertype=abstract

Tadmouri, A., Kiyonaka, S., Barbado, M., Rousset, M., Fablet, K., Sawamura, S., … De Waard, M. (2012). Cacnb4 directly couples electrical activity to gene expression, a process defective in juvenile epilepsy. *The EMBO Journal*, *31*(18), 3730–3744. http://doi.org/10.1038/emboj.2012.226

Takeuchi, O., & Akira, S. (2009). Innate immunity to virus infection, *227*, 75–86.

Takeuchi, O., & Akira, S. (2010). Pattern Recognition Receptors and Inflammation. *Cell*, *140*(6), 805–820. http://doi.org/10.1016/j.cell.2010.01.022

Tamura, T., Yanai, H., Savitsky, D., & Taniguchi, T. (2008). The IRF family transcription factors in immunity and oncogenesis. *Annual Review of Immunology*, *26*, 535–584. http://doi.org/10.1146/annurev.immunol.26.021607.090400

Taylor, J., Pereyra, a., Zhang, T., Messi, M. L., Wang, Z.-M., Herenu, C., … Delbono, O. (2014). The Cav 1a subunit regulates gene expression and suppresses myogenin in muscle progenitor cells. *The Journal of Cell Biology*, *205*(6), 829–846. http://doi.org/10.1083/jcb.201403021

Tessitore, a, Pastore, L., Rispoli, a, Cilenti, L., Toniato, E., Flati, V., … Martinotti, S. (1998). Two gamma-interferon-activation sites (GAS) on the promoter of the human intercellular adhesion molecule (ICAM-1) gene are required for induction of transcription by IFN-gamma. *European Journal of Biochemistry / FEBS*, *258*(3), 968–75. http://doi.org/10.1046/j.1432-1327.1998.2580968.x

Vendel, a. C. (2006). Alternative Splicing of the Voltage-Gated Ca2+ Channel beta4 Subunit Creates a Uniquely Folded N-Terminal Protein Binding Domain with Cell-Specific Expression in the Cerebellar Cortex. *Journal of Neuroscience*, *26*(10), 2635–2644. http://doi.org/10.1523/JNEUROSCI.0067-06.2006

Vendel, A. C., Rithner, C. D., & Lyons, B. a. (2006). Solution structure of the N-terminal A domain of the human voltage-gated Ca 2 + channel b 4a subunit, 378–383. http://doi.org/10.1110/ps.051894506.2000

Wali, J. P., Biswas, a, Chandra, S., Malhotra, a, Aggarwal, P., Handa, R., … Bahl, V. K. (1998). Cardiac involvement in Dengue Haemorrhagic Fever. *Int J Cardiol*, *64*(1), 31–36. http://doi.org/S0167-5273(98)00008-4 [pii]

Xu, X., Lee, Y. J., Holm, J. B., Terry, M. D., Oswald, R. E., & Horne, W. a. (2011). The Ca2+ Channel 4c Subunit Interacts with Heterochromatin Protein 1 via a PXVXL Binding Motif. *Journal of Biological Chemistry*, *286*(11), 9677–9687. http://doi.org/10.1074/jbc.M110.187864

Yacoub, S., Wertheim, H., Simmons, C. P., Screaton, G., & Wills, B. (2014). Cardiovascular manifestations of the emerging dengue pandemic. *Nature Reviews. Cardiology*, *11*(6), 335–45. http://doi.org/10.1038/nrcardio.2014.40

Yarovinsky, F., Zhang, D., Andersen, J. F., Bannenberg, G. L., Serhan, C. N., Hayden, M. S., … Sher, A. (2005). TLR11 activation of dendritic cells by a protozoan profilin-like protein. *Science (New York, N.Y.)*, *308*(5728), 1626–1629. http://doi.org/10.1126/science.1109893

Yoneyama, M., Kikuchi, M., Natsukawa, T., Shinobu, N., Imaizumi, T., Miyagishi, M., … Fujita, T. (2004). The RNA helicase RIG-I has an essential function in double-stranded RNA-induced innate antiviral responses. *Nature Immunology*, *5*(7), 730–737. http://doi.org/10.1038/ni1087

Young, P. R., Hilditch, P. a, Bletchly, C., & Halloran, W. (2000). An antigen capture enzyme-linked immunosorbent assay reveals high levels of the dengue virus protein NS1 in the sera of infected patients. *Journal of Clinical Microbiology*, *38*(3), 1053–7. Retrieved from http://www.pubmedcentral.nih.gov/articlerender.fcgi?artid=86336&tool=pmcentrez&rendertype=abstract

Zhang, Y., Yamada, Y., Fan, M., Bangaru, S. D., Lin, B., & Yang, J. (2010). The Subunit of Voltage-gated Ca2+ Channels Interacts with and Regulates the Activity of a Novel Isoform of Pax6. *Journal of Biological Chemistry*, *285*(4), 2527–2536. http://doi.org/10.1074/jbc.M109.022236